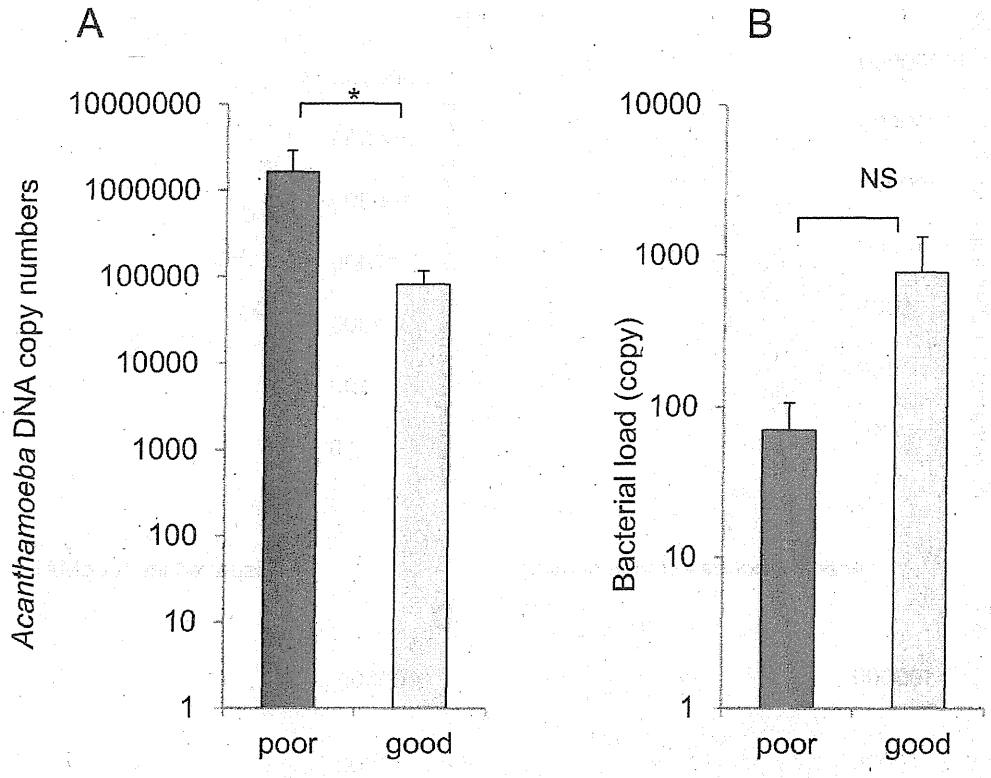

Figure 4. Elevation of *Acanthamoeba* DNA copy number in *Acanthamoeba* keratitis (AK) cases with poor outcomes. The AK cases with poor outcome, defined as visual acuity <20/50 at last visit or requiring keratoplasty, have a significantly higher number of *Acanthamoeba* DNA copies at the first visit compared with the AK eyes with good outcomes (**A**). Bacterial load at the first visit is not significantly different between them (**B**). *$P<0.05$. NS = not significant.

sessed by slit-lamp examinations.[4] The disease staging at presentation was predictive of worse outcomes and shown to help identify patients who might benefit from more aggressive therapy. Of note, advanced-stage AK with deep stromal involvement and ring infiltrates was associated with worse outcomes.[4,8,9]

Then, the important question arose on how much *Acanthamoeba* load is present at each stage. Our results showed that there was a strong and positive correlation of each stage with the *Acanthamoeba* DNA copy number, that is, more advanced stages of AK had higher *Acanthamoeba* DNA copy numbers. This explains why more advanced stages of AK were so refractory to treatment. Although the living amoebic bodies were fewer (Fig 1), this means that destroyed amoeba-derived DNA is abundant. Thus, the strong immunologic responses of the host to *Acanthamoeba*, manifested as ring infiltrate, are still not effective in eliminating the high *Acanthamoeba* copy numbers.

The most obvious advantage of real-time PCR is its high sensitivity.[3,10,11] Real-time PCR for *Acanthamoeba* genomic DNA will detect both live and destroyed amoeba. This was shown in our analysis of cultured *Acanthamoeba* cysts or trophozoites (Fig 1). Cultured *Acanthamoeba* samples generally are accompanied by fragments of the dead bodies and DNA. Real-time PCR attains its greater sensitivity in detecting

Table 1. Parameters Associated with Poor Outcome of *Acanthamoeba* Keratitis by Logistic Regression Analysis

	Odds Ratio					
	Lowest Category	*Second Category*	*95% CI*	*Highest Category*	*95% CI*	*P Value*
Acanthamoeba DNA copy number at the first visit	1.0	≤1000:3.48	1.04–111.63	>100 000:147.39	1.18–18 281.3	0.04*
AK stage	1.0	Stage 2:2.8	1.07–7.30	Stage 5:61.56	1.31–2838.69	0.04*
Bacterial load at the first visit	1.0	≤10:0.88	0.47–1.64	>10 000:0.53	0.02–11.86	0.69
Previous use of steroids	(-):1	8.84	0.852–91.68			0.07
Contact lens use	(-):1					0.996

AK = *Acanthamoeba* keratitis.
*$P\leq0.05$.

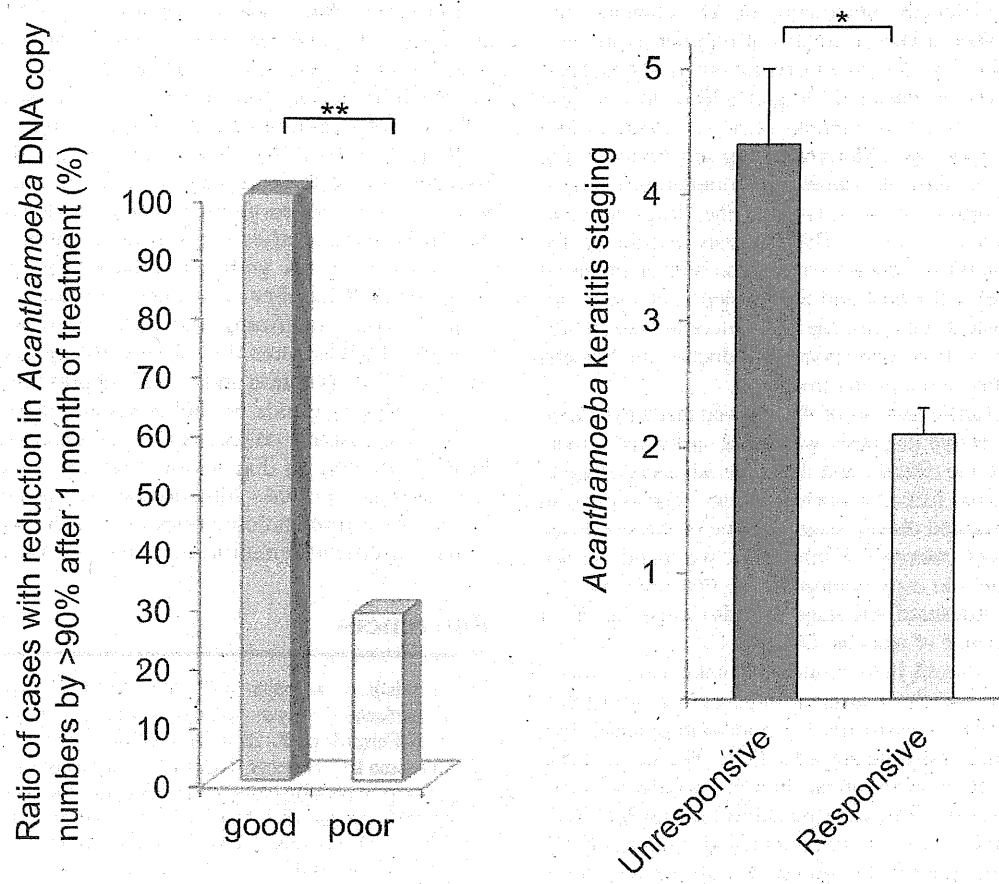

Figure 5. Association of poor outcomes with unresponsive *Acanthamoeba* copy reduction after treatment. Ratio of *Acanthamoeba* keratitis (AK) cases with unresponsive *Acanthamoeba* copy reduction after 1 month of treatment was significantly higher in AK with adverse prognosis (**A**). In the unresponsive AK cases, AK stage was significantly advanced compared with the responsive cases for amoebic copy reduction (**B**). $*P<0.01$. $**P=0.0005$.

Acanthamoeba because it does not rely on the functional integrity of the amoeba as do the conventional methods. The high sensitivity of the real-time PCR is also derived from the specificity of the TaqMan probe method[3] and the precise regression to the predetermined amount of amoebic DNA standards.

Even though *Acanthamoeba* is environmentally ubiquitous, our real-time PCR did not detect amoebic DNA in conjunctival smears from normal subjects. Although the number of subjects tested was limited, our findings indicate that amoebic trace is most likely absent in healthy eyes.

Acanthamoeba preys mainly on bacteria but also on fungi and other protozoans. Thus, *Acanthamoeba* might be observed as coinfectants in infectious keratitis cases. When we determined the specificity of *Acanthamoeba* PCR in BK cases, *Acanthamoeba* DNA was not detected in any of the BK cases, but 53.6% of the AK cases had low levels of bacterial DNA. This supports the concept of a bacterial involvement in the cause of AK, although the stage of the AK was not significantly correlated with the bacterial load (Fig 3). Thus, once AK is established, the bacterial load probably plays a limited role in its progression.

Table 2. Parameters Associated with Unresponsive *Acanthamoeba* DNA Reduction after 1 Month by Logistic Regression Analysis

	Odds Ratio					
	Lowest Category	*Second Category*	*95% CI*	*Highest Category*	*95% CI*	*P Value*
AK stage	1.0	Stage 2:8.00	1.06–58.82	Stage 5:4096	1.28–11 973 037	0.04*
Acanthamoeba DNA copy number at the first visit	1.0	≤1000:2.79	0.98–8	>100 000:60.88	0.92–4096	0.055
Bacterial load at the first visit	1.0	≤10:1.30	0.60–2.85	>10 000:6.52	2.99–14.25	0.51

AK = *Acanthamoeba* keratitis.
*$P \leq 0.05$.

In the course of lengthy treatments for AK, clinicians are often frustrated when a chosen treatment regimen is ineffective. In refractory cases, *Acanthamoeba* is sometimes resistant to antifungal drugs or antiseptic drugs. Indeed, in our case series, multidrug-resistant *Acanthamoeba* were detected especially in the refractory cases. Moreover, drug-sensitivity testing of *Acanthamoeba* in vitro takes weeks for completion and does not necessarily mirror the sensitivity to the drugs in vivo, especially in refractory cases.[12] This suggests that the proliferation of *Acanthamoeba* seems to depend on both an impaired immune response of the host and the virulence of the *Acanthamoeba*. Consistent with this, the AK outcome was significantly correlated with an unresponsive reduction of amoeba copy numbers after anti-amoeba treatment.

Previous multivariate analysis of AK showed that the duration of the symptoms before diagnosis was a risk factor for a more advanced stage of the disease, and the more advanced stage at presentation was a risk factor for worse outcome.[4] Consistent with these findings, advanced disease stage was one of the significant risk factors for poor outcomes. Furthermore, we found that the detected *Acanthamoeba* copy numbers at the first visit were another risk factor. Advanced AK stage was also a risk factor for unresponsive reduction of amoebic DNA.

Our findings should help clinicians make earlier decisions on when to switch to surgical intervention after treatment. Of note, risk assessments for poor outcomes do not necessarily require real-time amoebic PCR. We suggest that conventional PCR or even smear staining would be sufficient for this purpose. For example, careful sampling of AK lesions during the course of treatment and evaluations by conventional Calcofluor or Fungiflora Y staining will determine whether more than 90% of amoebic bodies have been cleared after 1 month of treatment.

The sensitivity of real-time PCR in patients with AK did not reach the theoretic 100% sensitivity that real-time PCR should have achieved, perhaps because the sampled amount was not sufficient and the sampled location was not correct. The staining of corneal lesions usually requires more tissues, and therefore staining samples were collected before sampling for PCR. When AK is at an early stage and has low amoebic numbers, the sampling may remove even trace amounts of *Acanthamoeba*. In this case, smear staining would be positive but PCR would be negative. The location or depth of the lesion may also affect its outcome. For example, when samples are obtained from inflammatory-prone lesions at the early stage, but without amoeba, real-time PCR would be negative.

The strong immune responses of the host also affect the amoebic DNA load. Aggressive AK treatment or presumably host factors would exacerbate the *Acanthamoeba* copy numbers. This can present as dense inflammatory opacities that are difficult to differentiate from AK with high levels of *Acanthamoeba*. Indeed, we had a case with low visual acuity due to severe corneal and anterior chamber inflammation, in which the small amount of amoebic DNA was readily eradicated after a few weeks of treatment, and treatment was successfully switched to topical steroid therapy to reduce the inflammatory responses.

Refractory AK cases sometimes require therapeutic keratoplasty. The management of post-keratoplasty cases requires intensive use of steroids because they are susceptible to rejection because of the larger graft size and strong inflammatory environment provoked by the AK.

Real-time PCR for *Acanthamoeba* is also useful for confirmation of the complete removal of *Acanthamoeba*. It is a great relief for surgeons to know that the amoebic DNA becomes negative after surgical intervention in cases with advanced-stage AK with a million copies. *Acanthamoeba* real-time PCR requires only a minute amount of sample and is useful for confirming the absence of *Acanthamoeba*. Amoebic PCR ensures the validity of aggressive treatment or surgical intervention and would support the proper timing for the use of steroids for better visual outcome.

In conclusion, collectively, *Acanthamoeba* real-time PCR is effective in diagnosing AK. Real-time PCR detection does not provide information on virulence of *Acanthamoeba* or immunologic responses of the host, but it does provide useful information in managing AK.

References

1. Shiraishi A, Kobayashi T, Hara Y, et al. Rapid detection of *Acanthamoeba* cysts in frozen sections of corneal scrapings with Fungiflora Y. Br J Ophthalmol 2009;93:1563–5.
2. MacLean RC, Hafez N, Tripathi S, et al. Identification of *Acanthamoeba* sp. in paraffin-embedded CNS tissue from an HIV+ individual by PCR. Diagn Microbiol Infect Dis 2007;57:289–94.
3. Riviere D, Szczebara FM, Berjeaud JM, et al. Development of a real-time PCR assay for quantification of *Acanthamoeba* trophozoites and cysts. J Microbiol Methods 2006;64:78–83.
4. Tu EY, Joslin CE, Sugar J, et al. Prognostic factors affecting visual outcome in *Acanthamoeba* keratitis. Ophthalmology 2008;115:1998–2003.
5. Kandori M, Inoue T, Takamatsu F, et al. Two cases of *Acanthamoeba* keratitis diagnosed only by real-time polymerase chain reaction. Cornea 2010;29:228–31.
6. Kakimaru-Hasegawa A, Kuo CH, Komatsu N, et al. Clinical application of real-time polymerase chain reaction for diagnosis of herpetic diseases of the anterior segment of the eye. Jpn J Ophthalmol 2008;52:24–31.
7. Nadkarni MA, Martin FE, Jacques NA, Hunter N. Determination of bacterial load by real-time PCR using a broad-range (universal) probe and primers set. Microbiology 2002;148:257–66.
8. Chew HF, Yildiz EH, Hammersmith KM, et al. Clinical outcomes and prognostic factors associated with *Acanthamoeba* keratitis. Cornea 2011;30:435–41.
9. Nguyen TH, Weisenthal RW, Florakis GJ. et al. Penetrating keratoplasty in active *Acanthamoeba* keratitis. Cornea 2010; 29:1000–4.
10. Thompson PP, Kowalski RP, Shanks RM, Gordon YJ. Validation of real-time PCR for laboratory diagnosis of *Acanthamoeba* keratitis. J Clin Microbiol 2008;46:3232–6.
11. Chang CW, Wu YC, Ming KW. Evaluation of real-time PCR methods for quantification of *Acanthamoeba* in anthropogenic water and biofilms. J Appl Microbiol 2010;109:799–807.
12. Perez-Santonja JJ, Kilvington S, Hughes R, et al. Persistently culture positive *Acanthamoeba* keratitis: in vivo resistance and in vitro sensitivity. Ophthalmology 2003;110:1593–600.

Footnotes and Financial Disclosures

Originally received: August 11, 2011.
Final revision: November 5, 2011.
Accepted: December 15, 2011.
Available online: March 3, 2012. Manuscript no. 2011-1207.

[1] Division of Ophthalmology and Visual Science, Faculty of Medicine, Tottori University, Tottori, Japan.

[2] Department of Ophthalmology, Ehime University School of Medicine, Ehime, Japan.

[3] Department of Ophthalmology, Kinki University Faculty of Medicine, Osaka, Japan.

[4] Department of Parasitology, National Institute of Infectious Diseases, Tokyo, Japan.

Financial Disclosure(s):
The author(s) have no proprietary or commercial interest in any materials discussed in this article.

Supported by a grant for research on emerging and reemerging infectious diseases from the Ministry of Health, Labor, and Welfare of Japan: H23-Shinko-Ippan-014. The funding organization had no role in the design or conduct of this research.

Correspondence:
Yoshifumi Ikeda, 81-859-38-6617, Division of Ophthalmology and Visual Science, Tottori University Faculty of Medicine, 36-1 Nishi-cho, Yonago 683-8504, Japan. E-mail: yoshifumiikeda@hotmail.com.

あたらしい眼科 29(3)：397～402，2012©

わが国のアカントアメーバ角膜炎関連分離株の分子疫学多施設調査（中間報告）

井上幸次[*1]　大橋裕一[*2]　江口　洋[*3]　杉原紀子[*4]　近間泰一郎[*5]　外園千恵[*6]
下村嘉一[*7]　八木田健司[*8]　野崎智義[*8]

[*1]鳥取大学医学部視覚病態学　[*2]愛媛大学大学院医学系研究科視機能外科学分野　[*3]徳島大学大学院ヘルスバイオサイエンス研究部眼科学分野　[*4]東京女子医科大学東医療センター眼科　[*5]広島大学大学院医歯薬学総合研究科視覚病態学
[*6]京都府立医科大学大学院医学研究科視覚機能再生外科学　[*7]近畿大学医学部眼科学教室　[*8]国立感染症研究所寄生動物部

Multicenter Molecular Epidemiological Study of Clinical Isolates Related with *Acanthamoeba* Keratitis (Interim Report)

Yoshitsugu Inoue[1)], Yuichi Ohashi[2)], Hiroshi Eguchi[3)], Noriko Takaoka-Sugihara[4)], Tai-ichiro Chikama[5)], Chie Sotozono[6)], Yoshikazu Shimomura[7)], Kenji Yagita[8)] and Tomoyoshi Nozaki[8)]

[1)] *Division of Ophthalmology and Visual Science, Faculty of Medicine, Tottori University,* [2)] *Department of Ophthalmology, Graduate School of Medicine, Ehime University,* [3)] *Department of Ophthalmology, Institute of Health Biosciences, The University of Tokushima Graduate School,* [4)] *Department of Ophthalmology, Tokyo Women's Medical University Medical Center East,* [5)] *Department of Ophthalmology and Visual Science, Hiroshima University Graduate School of Biomedical Sciences,* [6)] *Department of Ophthalmology, Kyoto Prefectural University of Medicine,* [7)] *Department of Ophthalmology, Kinki University Faculty of Medicine,* [8)] *Department of Parasitology, National Institute of Infectious Diseases*

目的：角膜炎に関連したアカントアメーバのDNA分子を多施設疫学研究として解析する．**方法**：全国6施設で，アカントアメーバ角膜炎に関連して分離されたアメーバ株をクローニング後，18S ribosomal RNA遺伝子のシークエンス解析を行った．そして，BLAST (basic local alignment search tool) 検索による既存アメーバとの相同性を調べ，Tタイピングによる分類を行った．本研究は現在も継続中であるが，最初の2年間の結果を中間報告としてまとめた．**結果**：43株〔角膜擦過物27株，保存液15株，MPS (multi-purpose solution) ボトル内液1株〕中42株がT4に分類され，角膜由来の1株のみT11に分類された．角膜分離株のシークエンスタイプは15種類に分かれたが，すべて既知のものと一致した．保存液分離株のタイプは10種類に分かれ，角膜分離株と比較できた9株中6株は角膜分離株と一致した．**結論**：最近のアカントアメーバ角膜炎のわが国での増加は，新たなシークエンスタイプのアメーバの出現によるものではなく，既存の株による感染の増加である．

Objective：To analyze *Acanthamoeba* DNA molecule's relationship to keratitis, in a multicenter epidemiological study. **Method**：*Acanthamoeba* keratitis-related isolates from 6 institutes were cloned, and sequences of the 18S ribosomal RNA gene were analyzed. Homology between them and known sequences was then examined using BLAST (basic local alignment search tool), and they were classified by T typing. This research is still ongoing; the results of the first two years have been analyzed as an interim report. **Results**：Of 43 isolates, including 27 isolates from the cornea, 15 from lens cases and 1 from an MPS (multi-purpose solution) bottle, 42 isolates were classified as T4; only 1 was classified as T11. Sequences were classified into 15 types; none were unique genotypes. Sequences of isolates from lens cases were classified into 10 types; of the 9 isolates with which corneal isolates had also been obtained, the sequences of 6 were identical with the sequences of the corneal isolates. **Conclusion**：These results indicate that the recent increase of *Acanthamoeba* keratitis incidence in Japan is not due to the emergence of novel amoebic genotypes, but to increased incidence of infection by known genotypes.

〔Atarashii Ganka (Journal of the Eye) **29**(3)：397～402，2012〕

〔別刷請求先〕井上幸次：〒683-8504 米子市西町36-1　鳥取大学医学部視覚病態学
Reprint requests：*Yoshitsugu Inoue, M.D., Ph.D., Division of Ophthalmology and Visual Science, Faculty of Medicine, Tottori University, 36-1 Nishi-cho, Yonago 683-8504, JAPAN*

0910-1810/12/¥100/頁/JCOPY

Key words：アカントアメーバ角膜炎，分子疫学，Tタイピング，18S ribosomal RNA，多施設共同研究．*Acanthamoeba* keratitis, molecular epidemiology, T typing, 18S ribosomal RNA, multicenter study.

はじめに

アカントアメーバは土壌・水中をはじめ自然界に広く生息する原虫であり，水道水からも検出される．アカントアメーバにより角膜炎を発症することは1974年にはじめて報告された[1]が，本来は外傷に伴う非常にまれな感染症であった．しかし，その後コンタクトレンズ（CL）装用に伴う感染として認められるようになり，わが国では1988年に石橋らがはじめて報告した[2]．当初はそれでもまれな疾患であったが，CL保存に水道水を用いることのできたソフィーナ®での感染が多いことが注目されるようになり，その後しだいに報告が増加し，特に2006年頃からは急速に増えて，従来報告のなかった北海道や東北でも症例が報告されるようになった．2007年4月～2009年3月にかけて行われたコンタクトレンズ関連角膜感染症の全国調査[3]でも，入院を必要としたCL関連角膜感染症の2大起炎菌として緑膿菌とともに浮かび上がった．その多くが，multi-purpose solution（MPS）をケア用品として使用している頻回交換型のCLユーザーであり，MPSのアカントアメーバに対する効果が低いことが検証されるとともに，CLユーザーの最大の合併症として，その診断・治療や予防対策の重要性が高まっている．

このような状況のなかで，わが国のアカントアメーバ角膜炎（AK）の原因となっているアメーバの感染源・感染経路，アメーバ感染の地域差や年次動向，アメーバ株と臨床所見・治療への反応性・予後との関係を疫学的に調べる必要性が生じてきた．アカントアメーバを疫学的に分類・比較するにあたって，形態学的に分類することはもちろん重要だが，培養条件によって，形態を変化させるアカントアメーバの場合，限界があり，現在は，アカントアメーバのDNAを利用して分子遺伝学的に分類，同定することが主流となっている．

アカントアメーバの遺伝子型別の方法としてはTタイピングが用いられている．これは1996年Gastらにより提唱され，18S ribosomal RNA（18S rRNA）をコードしているDNAを用いて行われる[4]．この方法では2つのシークエンスを全長比較して相同性が5%以上違う場合，別々のTタイプと分類される．現在15のタイプがあり，1つのTタイプには多種類のシークエンスが含まれる．これまでT1-T6，T10-T12のアメーバが角膜炎あるいはアメーバ性脳炎より検出されている．タイピングは特定の集団と疾患との関連を調べるうえできわめて有用である．

今回，筆者らは先に述べたコンタクトレンズ関連角膜感染症調査研究班の施設を中心に多施設からのアカントアメーバ株を国立感染症研究所寄生動物部に集積し，Tタイピングによる解析を行った．この研究は厚生労働省の新興・再興感染症研究事業の一環として行われており，現在も参加施設を増やして継続中であるが，本報告では最初の2年の結果を中間報告としてまとめる．

I 対象および方法

1. 対　　象

対象は，全国の6施設（鳥取大学，愛媛大学，徳島大学，東京女子医科大学東医療センター，山口大学，京都府立医科大学）の眼科に2009年4月～2010年12月の間に受診したAK患者の角膜擦過物，CLケース（保存液），MPSボトル，使用環境（洗い場）から分離されたアカントアメーバ株および，これらの施設で過去に分離され，保存されていた株を対象とした．本研究については，各施設の倫理委員会にかけて了承を得，過去に分離された株も含めて，本研究に使用することを患者本人あるいは代諾者に文書で承諾を得た．

角膜擦過物から27株，CLケース（保存液）から15株，MPSボトルから1株，計43株が対象である．

2. アカントアメーバの培養と無菌クローン化

アカントアメーバは大腸菌を塗布した1.5% non-nutrient agar（NN培地）上で25℃にて分離，培養した．これをキャピラリーピペットによる釣り上げ法（micro-manipulation法）にて単離し，さらに大腸菌寒天培地上でクローン培養した[5]．

無菌化の手順としては，クローン化したアカントアメーバのシストを1 m*l*の0.1N塩酸溶液中で，37℃にて一晩処理を行った後，500×g，5分間遠心分離を行ってシストを沈殿させた．その後，塩酸を除去して滅菌蒸留水に浮遊させ，同じ条件で再度遠心を行った．滅菌蒸留水を除去し，得られたシストを100単位/mLのペニシリン（明治製菓）と，100 μg/mLのストレプトマイシン（明治製菓）を添加し，PYGC培地（10 g/L Proteose peptone, 5 g/L NaCl, 10 g/L Yeast extract, 10 g/L Glucose, 0.95 g/L L-Cysteine, 10 mM Na_2HPO_4, 5 mM KH_2PO_4）で培養した[5]．

3. DNA解析

遺伝子抽出キットQIAamp® DNA Mini Kit〔(株) キアゲン〕を使用して，添付のプロトコールに従ってDNAを抽出した．

抽出したアメーバDNAを，GeneAmp® PCR (polymerase chain reaction) system 2400により，アメーバ特異プライマーであるJDP1-JDP2を用い，18S rRNA遺伝子の高可変領域の一つであるDF3 (diagnostic fragment 3) を含む約

400塩基対を既報の温度条件で増幅した[6].

PCRにて増幅された産物の塩基配列を蛍光シークエンサー(ABI PRISM® 310 Genetic Analyzer)を用いて,シークエンス用プライマー892Cにより解析した[6].

4. ホモロジー検索

このようにして得られた塩基配列をBLAST (basic local alignment search tool)を用いてGenBank, EMBL (European Molecular Biology Laboratory), DDBJ (DNA Data Bank of Japan)に登録された株と照合した.データベースに登録された株で,対象株と相同性の最も高いものを検索し,データベース登録名,対象株と登録株との相同性,登録株の分離元を調べた.

5. 系統樹作製

対象株とデータベースに登録されているTタイピング(T1～T15)の代表的な株を用いて,解析用プログラムとしてClustal Wを用いて系統樹を作製した.

II 結　果

1. 角膜分離27株ホモロジー検索の結果

角膜分離27株のTタイピングの結果では1株のみがT11であったが,他はT4であった(96.3%).T4に属する26株のうち22株は角膜炎より分離されている既知の配列と一致し,それ以外の4株は角膜炎分離株では認められないもののやはり既知の配列と一致した(表1).

ホモロジー検索の結果をもとに,系統樹を描く(図1)とT4の中で特定の遺伝的集団を形成せず,遺伝的には多様性を認め15種類に分かれた.そのうち,複数株,複数地域に検出されるシークエンスのタイプとして,ATCC30461 Eye strainやATCC50497 Rowdon strainなどと相同性を認めるものが存在した(図2).

2. CLケース(保存液)由来株・MPSボトル由来株と角膜分離株の関係(表2)

保存液分離株15株のシークエンスはすべてT4であったが,10種類のシークエンスタイプに分かれた.このタイプでは,患者の角膜分離株とともに分離された9組中6組は一致したが,3組では一致しなかった.MPSボトル由来の1株についてはその患者の角膜分離株およびCLケース(保存液)由来株の3者のシークエンスタイプが一致した.

表1　アカントアメーバ角膜炎患者の角膜擦過物由来株の18S rRNA遺伝子タイピング

由来	試料ID	T type	BLASTで相同性の高かった(99-100%)株の配列	左記配列の分離試料
角膜	1-1-1	T4	ATCC50497 *Acanthamoeba* sp. Rowdon strain	Keratatis
角膜	1-2-1	T4	ATCC50497 *Acanthamoeba* sp. Rowdon strain	Keratatis
角膜	1-3-1	T4	*Acanthamoeba* sp. S2JDP	Soil
角膜	1-5-1	T4	ATCC30461 *A. polyphaga* Eye strain	Keratatis
角膜	1-6-1	T4	ATCC50497 *Acanthamoeba* sp. Rowdon strain	Keratatis
角膜	1-7-1	T4	*Acanthamoeba* sp. KA/E10	Keratatis
角膜	1-8-1	T4	*Acanthamoeba* sp. KA/E6	Keratatis
角膜	1-9-1	T4	*Acanthamoeba* sp. Vazaldua	Keratatis
角膜	3-1-1	T4	*Acanthamoeba* sp. CDC #V390	Brain, Skin
角膜	3-2-1	T4	ATCC30461 *A. polyphaga* Eye strain	Keratatis
角膜	3-3-1	T4	ATCC 50370 *A. castellanii* Ma strain	Keratatis
角膜	3-4-1	T4	ATCC 50374 *A. castellanii* Castellani	Yeast culture
角膜	3-7-1	T4	ATCC 50370 *A. castellanii* Ma strain	Keratatis
角膜	4-1-1	T4	*Acanthamoeba* sp. CDC # V390	Brain, Skin
角膜	4-3-1	T4	ATCC50497 *Acanthamoeba* sp. Rowdon strain	Keratatis
角膜	4-4-1	T4	ATCC30461 *A. polyphaga* Eye strain	Keratatis
角膜	4-5-1	T4	*A. castellanii* CDC #V042	Keratatis
角膜	6-2-1	T4	ATCC30461 *A. polyphaga* Eye strain	Keratatis
角膜	6-5-1	T4	ATCC30461 *A. polyphaga* Eye strain	Keratatis
角膜	7-1-1	T11	*A. hatchetti* 4RE	Keratatis
角膜	7-2-1	T4	*Acanthamoeba* sp. KA/E24	Keratatis
角膜	7-3-1	T4	*Acanthamoeba* sp. KA/E6	Keratatis
角膜	7-4-1	T4	*Acanthamoeba* sp. UIC 1060 voucher	Keratatis
角膜	7-5-1	T4	*Acanthamoeba* sp. CDC #V014	Keratatis
角膜	9-1-1	T4	*Acanthamoeba* sp. CDC #V062	Keratatis
角膜	9-2-1	T4	*Acanthamoeba castellanii* CDC #V042	Keratatis
角膜	9-3-1	T4	*Acanthamoeba* sp. KA/E6	Keratatis

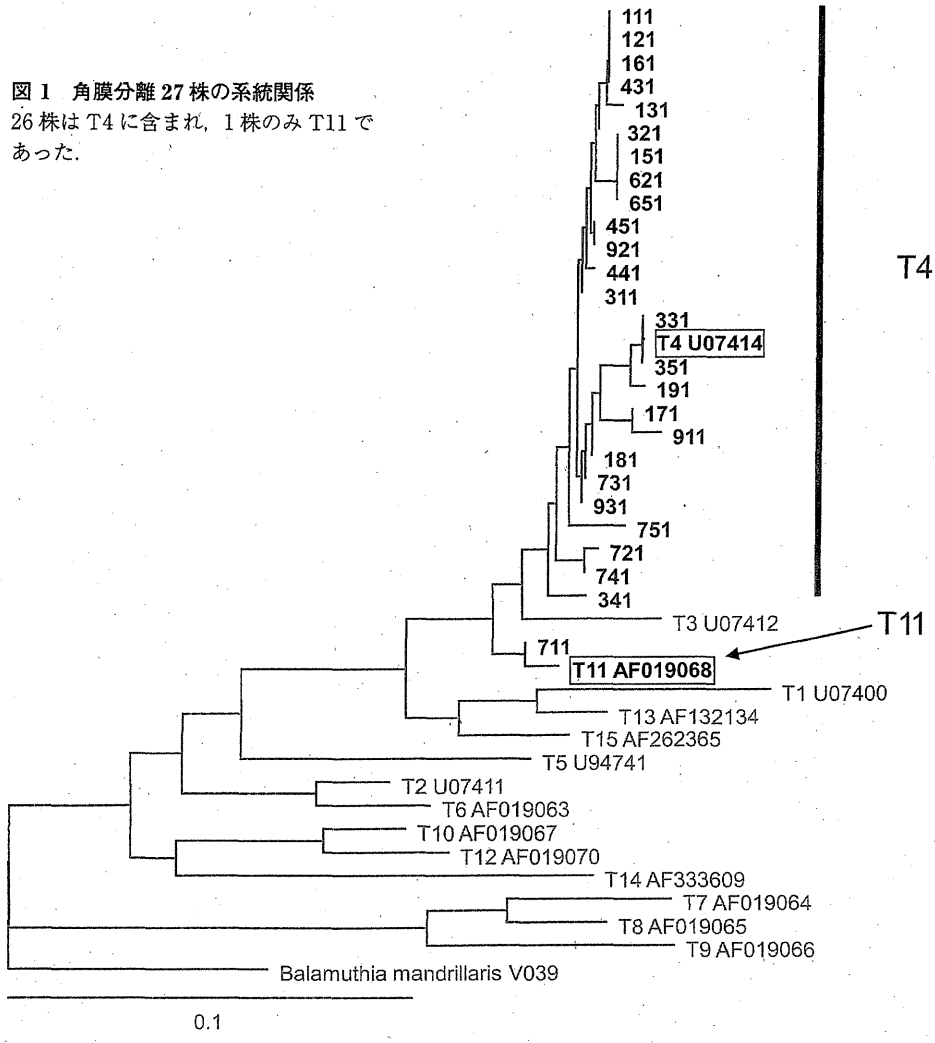

図 1　角膜分離 27 株の系統関係
26 株は T4 に含まれ，1 株のみ T11 であった．

表 2　アカントアメーバ角膜炎患者のレンズケース（保存液）・MPS ボトル・使用環境（洗い場）由来株の 18S rRNA 遺伝子タイピングと角膜由来株との一致性

試料	試料 ID	T type	BLAST で相同性の高かった（99-100%）株の配列	左記配列の分離試料	角膜分離株との一致性
保存液	1-3-2	T4	*Acanthamoeba* sp S2JDP	Soil	一致
保存液	1-4-2	T4	*Acanthamoeba* sp. S15	Keratatis	不明
保存液	1-5-2	T4	ATCC30461 *A. polyphaga* Eye strain	Keratatis	一致
保存液	1-6-2	T4	ATCC50497 *Acanthamoeba* sp. Rowdon strain	Keratatis	一致
保存液	1-7-2	T4	*Acanthamoeba* sp. KA/E10	Keratatis	一致
保存液	3-1-2	T4	*Acanthamoeba* sp. KA/E6	Keratatis	不一致
保存液	3-2-2	T4	*Acanthamoeba* sp. CDC #V390	Keratatis	不一致
保存液	3-5-2	T4	*Acanthamoeba* sp. KA/E6	Keratatis	一致
保存液	4-2-2	T4	*Acanthamoeba* sp. CDC # V390	Brain, Skin	不明
保存液	6-1-3	T4	*Acanthamoeba* sp. CDC #V062	Keratatis?	不明
保存液	6-2-2	T4	ATCC30461 *A. polyphaga* Eye strain	Keratatis	一致*
保存液	6-5-2	T4	*Acanthamoeba* sp. CDC #V014	Keratatis	不一致
保存液	6-10-2	T4	ATCC30461 *A. polyphaga* Eye strain	Keratatis	不明
保存液	6-11-2	T4	*Acanthamoeba* sp. KA/E10	Keratatis	不明
保存液	9-4-1	T4	*Acanthamoeba* sp. CDC #V042	Keratatis	不明
MPS	6-2-3	T4	ATCC30461 *A. polyphaga* Eye strain	Keratatis	一致*

*角膜とレンズケース（保存液）とケア用品の 3 者で一致．

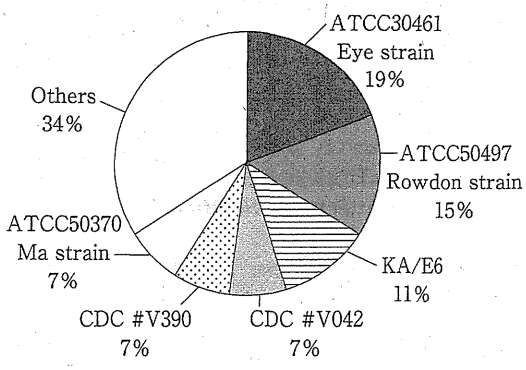

図2　シークエンスタイプの検出頻度
多くのタイプが認められたが，Eye strain 次いで Rowdon strain が多かった．

III　考　　按

AKの原因となったアメーバのTタイピングについてはすでに各国から報告がなされており，わが国でも高岡らの報告がある[5]が，今回のように多施設で広く日本の株を集めて行われたスタディははじめてである．

今回の報告では1株を除いてすべてをT4が占めており，これは過去の多くの報告と一致している．たとえば，Ledeeら[7]は米国フロリダ州のAK患者のサンプル37株のうち36株がT4，1株のみT5であったと報告している．一方，Yeraら[8]はフランスのアカントアメーバ分離株37株のうち，AK患者由来の10株はすべてT4であったとしている．ただし，それ以外のCL使用者のCL，保存液でも79%がT4であるとしており，臨床的に重要なT4はもともと環境中に最も多く認められるグループである（半数以上）ことには留意が必要であり[9]，より多くの環境に適応しうる能力をもっていると考えられ，そのため保存液中で生存しやすく，さらにはアカントアメーバにとって決して住みやすいとは言いがたい角膜でも生存しうるのではないかと推察される．

今回のスタディでは1株のみT11が認められたが，T11が角膜炎を発症するという報告は過去にもすでにあり[10]，本研究のこの症例（試料ID 7-1-1）が特に他の症例と比較して臨床所見に特徴があるとか，難治であるとかいうことはなかった（データ示さず）．また，今回のスタディには1例，非CL装用者の症例が含まれており（試料ID 1-2-1），感染経路は不明で1カ月ほどの間に急速に進行して穿孔し，治療的角膜移植を要したが，この症例も分類上はT4で，しかも今回2番目に多いサブタイプであるRowdon strainに含まれていた（データ示さず）．インドではCLと関係ないAK患者が多いが，分離株はやはりT4であることが報告されており[11]，CLとT4との間に特別の結びつきがあるわけではないようである．

T4の中のサブタイプで，Eye strainの患者5名は愛媛・徳島・岡山・静岡と瀬戸内および太平洋側に分布しており，Rowdon strainの4名は鳥取・京都の患者で，日本海側であった（データ示さず）．これが地域差を示すものか，偶然のものかは個々のグループの株数が少ないため，結論できないが，興味深い傾向であり，株数を増やして解析を続け，明らかにしていきたい．

感染症の分子サーベイランスの効能として，高病原性株や薬剤抵抗株の発生監視やアウトブレーク時の迅速な要因解明と感染拡大の阻止があり，AKでもこれが一つの重要な目的となる．たとえば，米国シカゴ周辺で上水道の消毒の方法が変更になったことに伴って生じたと推測されるAKのアウトブレーク（2003～2005年）の株を解析した報告があり[12]，87%がT4，13%がT3であったが，アカントアメーバ角膜炎からの分離株として報告されたことのない新たなシークエンスタイプの株は見つからなかったとしている．また，Zhangら[13]は中国北部のAK患者からのアカントアメーバは26株中25株はT4，1株はT3だったが，18株（69.2%）はユニーク・シークエンスだったとしている．今回，わが国のAKの増加を受けて，解析を行ったが，新たなシークエンスタイプは見つからず，特定のシークエンスタイプへの集積も認められなかった．

本報告で，角膜とCLケース（保存液）の株を比較できた9例のうち，6例はシークエンスタイプが一致しており，これは十分予想されることであったが，3例においては不一致であった．これをどう考えるかであるが，一つはCLケース（保存液）に複数の株が汚染しており，そのうちの一つが角膜に感染を起こし，別の一つが保存液から分離された可能性である．もう一つの可能性として，不一致例では，角膜感染株はCL保存液でなく，CLを使用している洗い場などの環境由来と考えることもできる．Bootonら[14]は香港のAK患者の角膜擦過物と家の水道水から分離された株は一致しなかったとしている．今回の筆者らの検討では使用環境（洗い場）由来株が1株しかなく，かつその症例では角膜から分離ができていないため，本報告からは除外した．今後，環境由来株も増やして，角膜由来株との一致性について検討していきたい．

本研究では，アカントアメーバ分子疫学を行うにあたって，アメーバ株のクローン化と無菌化を行ったが，このように，分離株を保存し，研究資源として活用していくうえでも分子疫学は有用である．

今回の分子疫学により，国内AKの起因アメーバのほとんどはT4タイプであったが，特定のシークエンスのタイプには収束せず，近年のわが国のAK増加は，新たな高病原性タイプあるいは株の出現ではなく，以前から環境中に生息していたT4中の多くのシークエンスタイプのアメーバの感染リスクが増加したものであると考えられた．いくつかのシ

ークエンスタイプの異なるアメーバが角膜より高頻度で検出されたが，アメーバ自体の生物学的特性の関与か，地域性（環境，温度など）の違いなのかは不明である．

アカントアメーバについては病原因子の解析が十分ではなく，細胞表面への付着に関与するマンノース結合性蛋白や蛋白分解酵素の関与がいわれている[15,16]ものの，Tタイピングがそのような性質や病原性と関連するかどうかもまだよくわかっていない．今後は，参加施設数を増やしてアメーバ株をさらに集積し，使用環境からの分離株も増やして分子疫学を継続・拡大し，感染経路，地域差や温暖化による影響などについて検討するとともに，アメーバ株に対する薬剤感受性試験を行い，臨床所見とも比較することによって，臨床病型や治療経過との関連についても検討を加えていく予定である．

本研究は厚生労働科学研究費補助金　新興・再興感染症研究事業「顧みられない病気に関する研究」「顧みられない寄生虫病の効果的監視法の確立と感染機構の解明に関する研究」の分担研究として行われた．

以下のコンタクトレンズ関連角膜感染症全国調査委員会委員の先生方に多くの有益なご助言をいただきました．ここに深謝致します．

石橋康久（東鷲宮病院眼科），植田喜一（ウエダ眼科），稲葉昌丸（稲葉眼科），宇野敏彦（愛媛大学），田川義継（北海道大学），福田昌彦（近畿大学）．（敬称略）

文　献

1) Naginton J, Watson PG, Playfair TJ et al：Amoebic infection of the eye. *Lancet* **2**：1537-1540, 1974
2) 石橋康久，松本雄二郎，渡辺亮子ほか：Acanthamoeba keratitis の1例―臨床像，病原体検査法および治療についての検討―．日眼会誌 **92**：963-972, 1988
3) 宇野敏彦，福田昌彦，大橋裕一ほか：重症コンタクトレンズ関連角膜感染症全国調査．日眼会誌 **115**：107-115, 2011
4) Gast RJ, Ledee DR, Fuerst PA et al：Subgenus systematics of *Acanthamoeba*：four nuclear 18S rDNA sequence types. *J Eukaryot Microbiol* **43**：498-504, 1996
5) 高岡紀子，八木田健司，山上　聡ほか：当院で得られたアカントアメーバの遺伝学的分類．眼科 **52**：1811-1817, 2010
6) Schroeder JM, Booton GC, Hay J et al：Use of subgenic 18S ribosomal DNA PCR and sequencing for genus and genotype identification of Acanthamoebae from humans with keratitis and from sewage sludge. *J Clin Microbiol* **39**：1903-1911, 2001
7) Ledee DR, Iovieno A, Miller N et al：Molecular Identification of T4 and T5 genotypes in isolates from *Acanthamoeba* keratitis patients. *J Clin Microbiol* **47**：1458-1462, 2009
8) Yera H, Zamfir O, Bourcier T et al：The genotypic characterisation of *Acanthamoeba* isolates from human ocular samples. *Br J Ophthalmol* **92**：1139-1141, 2008
9) Booton GC, Visvesvara GS, Byers TJ et al：Identification and distribution of *Acanthamoeba* species genotypes associated with nonkeratitis infections. *J Clin Microbiol* **43**：1689-1693, 2005
10) Lorenzo-Morales J, Morcillo-Laiz R, Lopez-Velez R et al：*Acanthamoeba* keratitis due to genotype T11 in a rigid gas permeable contact lens wearer in Spain. *Contact Lens Anterior Eye* **34**：83-86, 2011
11) Sharma S, Pasricha G, Das D et al：*Acanthamoeba* keratitis in non-contact lens wearers in India. DNA typing-based validation and a simple detection assay. *Arch Ophthalmol* **122**：1430-1434, 2004
12) Booton GC, Joslin CE, Shoff M et al：Genotypic identification of *Acanthamoeba* sp. isolates associated with an outbreak of *Acanthamoeba* keratitis. *Cornea* **28**：673-676, 2009
13) Zhang Y, Sun X, Wang Z et al：Identification of 18S ribosomal DNA genotype of *Acanthamoeba* from patients with keratitits in North China. *Invest Ophthalmol Vis Sci* **45**：1904-1907, 2004
14) Booton GC, Kelly DJ, Chu Y-W et al：18S ribosomal DNA typing and tracking of *Acanthamoeba* species isolates from corneal scrape specimens, contact lenses, lens cases, and home water supplies of *Acanthamoeba* keratitis patients in Hong Kong. *J Clin Microbiol* **40**：1621-1625, 2002
15) Cao Z, Jefferson DM, Panjwani N：Role of carbohydrate-mediated adherence in cytopathogenic mechanisms of *Acanthamoeba*. *J Biol Chem* **273**：15838-15845, 1998
16) Hurt M, Niederkorn J, Alizadeb, H：Effects of mannose on *Acanthamoeba castellanii* proliferation and cytolytic ability to corneal epithelial cells. *Invest Ophthalmol Vis Sci* **44**：3424-3431, 2003

*　　*　　*

Biochemical and Biophysical Research Communications 415 (2011) 421–425

Contents lists available at SciVerse ScienceDirect

Biochemical and Biophysical Research Communications

journal homepage: www.elsevier.com/locate/ybbrc

Identification of a second catalytically active trans-sialidase in *Trypanosoma brucei*

Fumiki Nakatani [a,1,2], Yasu S. Morita [a,b,*,1], Hisashi Ashida [a,3], Kisaburo Nagamune [a,4], Yusuke Maeda [a,b], Taroh Kinoshita [a,b]

[a] *Department of Immunoregulation, Research Institute for Microbial Diseases, Osaka University, Osaka, Japan*
[b] *Department of Immunoglycobiology, WPI Immunology Frontier Research Centre, Osaka University, Osaka, Japan*

ARTICLE INFO

Article history:
Received 1 October 2011
Available online 21 October 2011

Keywords:
Glycosylphosphatidylinositol
Procyclin
Sialic acid
Sleeping sickness
trans-Sialidase
Trypanosoma brucei

ABSTRACT

The procyclic stage of *Trypanosoma brucei* is covered by glycosylphosphatidylinositol (GPI)-anchored surface proteins called procyclins. The procyclin GPI anchor contains a side chain of *N*-acetyllactosamine repeats terminated by sialic acids. Sialic acid modification is mediated by trans-sialidases expressed on the parasite's cell surface. Previous studies suggested the presence of more than one active trans-sialidases, but only one has so far been reported. Here we cloned and examined enzyme activities of four additional trans-sialidase homologs, and show that one of them, *Tb927.8.7350*, encodes another active trans-sialidase, designated as TbSA C2. In an *in vitro* assay, TbSA C2 utilized α2-3 sialyllactose as a donor, and produced an α2-3-sialylated product, suggesting that it is an α2-3 trans-sialidase. We suggest that TbSA C2 plays a role in the sialic acid modification of the trypanosome cell surface.

1. Introduction

Trypanosoma brucei is a protozoan parasite responsible for African sleeping sickness in humans and a disease called nagana in livestock. It is transmitted by an insect vector, the tsetse fly. The procyclic stage *T. brucei* proliferates in the midgut of the tsetse fly, and is covered by glycosylphosphatidylinositol (GPI)-anchored proteins termed procyclins [1]. The GPI anchor of procyclins is modified by a complex poly-*N*-acetyllactosamine side chain, which contains sialic acids as terminal residues [2,3].

Despite the presence of sialylated glycoconjugates on its cell surface, *T. brucei* is unable to synthesize sialic acids *de novo*. The parasite is therefore totally dependent on exogenous sialoglycoconjugates available in the tsetse fly midgut to sialylate procyclins. In order to scavenge sialic acids from the environment, the parasite expresses trans-sialidases that can transfer sialic acids from host-derived sialoglycoconjugates to terminal β-galactose residues of the GPI side chain by a transglycosylation reaction [4–6].

Trans-sialidases are expressed on the parasite's surface as GPI-anchored proteins [4,5]. Compared with procyclins, which are major GPI-anchored proteins, trans-sialidases account for only a small proportion of the GPI-anchored proteins. We have previously generated mutant *T. brucei* deficient in GPI precursor biosynthesis, by deleting the third mannosyltransferase gene, *TbGPI10* [7]. These mutants synthesize truncated GPIs that are structurally defective in anchoring proteins, but can still be expressed on the cell surface as free (unanchored) GPIs, after being elaborated by a poly-*N*-acetyllactosamine side chain. Strikingly, the side chains of such truncated GPIs were modified by sialic acids because of secreted trans-sialidases. In the absence of the GPI precursor, GPI transamidase, which is intact in *TbGPI10* knockout mutants, mediates the hydrolysis of the hydrophobic GPI anchoring signal at the C-terminus of nascent proteins. The mutant consequently secretes GPI-anchored proteins as soluble forms. trans-Sialidases are therefore secreted into the extracellular milieu, where they can function to elaborate the GPI side chain. This mutant was able to proliferate in the tsetse fly midgut, though less effectively than wild-type parasites, suggesting that free GPI with sialylated side chains was sufficient for the survival and growth of the parasite in the midgut [7,8].

In order to determine if sialic acid was critical for the parasite's survival in the midgut, we took advantage of another GPI biosynthetic mutant that is defective in *TbGPI8* [9], the catalytic component of GPI transamidase. The *TbGPI8* deletion mutant accumulates non-protein-linked GPI molecules, and some of these free GPIs are

Abbreviations: GPI, glycosylphosphatidylinositol; ORF, open reading frame; TLC, thin layer chromatography.

* Corresponding author at: Department of Immunoregulation, Research Institute for Microbial Diseases, Osaka University, 3-1 Yamada-oka, Suita, Osaka 565-0871, Japan. Fax: +81 6 6875 5233.
E-mail address: ymorita@biken.osaka-u.ac.jp (Y.S. Morita).
[1] These authors contributed equally to this work.
[2] Current address: Department of Applied Life Sciences, Graduate School of Life and Environmental Sciences, Osaka Prefecture University, Osaka, Japan.
[3] Current address: Division of Integrated Life Science, Graduate School of Biostudies, Kyoto University, Kyoto 606-8502, Japan.
[4] Current address: Department of Parasitology, National Institute of Infectious Diseases, Shinjuku-ku, Tokyo 162-8640, Japan.

0006-291X/$ - see front matter © 2011 Elsevier Inc. All rights reserved.
doi:10.1016/j.bbrc.2011.10.085

located on the cell surface [10]. However, in contrast to the *TbGPI10* mutant that can secrete an unanchored form of trans-sialidases, the *TbGPI8* mutant cannot cleave the GPI-anchor signal, and nascent proteins are therefore unable to be secreted [8]. These nascent proteins are presumably degraded intracellularly. As a consequence, complete GPI precursors elaborated by poly-*N*-acetyllactosamine side chains are produced, but not sialylated, due to the lack of trans-sialidases. The growth of *TbGPI8* mutants was severely compromised in the tsetse fly midgut [8,10], and we therefore suggested that sialic acid was essential for the growth of the procyclic form of the parasites in the fly midgut [8].

We expressed a known trans-sialidase (*i.e.* TbTS encoded by *Tb927.7.6850*) as a soluble form in the *TbGPI8* knockout mutant in an attempt to restore the proliferation of parasites in the midgut. This complemented strain regained the ability to sialylate surface-exposed free GPIs, and showed an improved rate of proliferation in the midgut. However, the level of infection was lower than that achieved by *TbGPI10* knockout parasites [8].

One possible explanation for these results is that TbTS is not the only trans-sialidase involved in GPI side chain modification. There are nine homologs in the *T. brucei* genome database [6,11] (and this study). A recent report suggested that TbSA C is a sialidase, rather than a trans-sialidase [11]. However, there have been no reports of any other functional trans-sialidases in *T. brucei*. We cloned and expressed a number of these trans-sialidase homologs, and examined their ability to function as trans-sialidase enzymes. Contrary to the previous report, our data indicate that TbSA C is an active trans-sialidase, suggesting that it may be a critical enzyme that works together with TbTS to elaborate the GPI side chains.

2. Materials and methods

2.1. Cell strains and culture

The procyclic form of *T. brucei* strain 427 was used in this study. *TbGPI10* and *TbGPI8* knockout mutants were previously established [7,9]. To create trans-sialidase expression cell lines, the plasmids (50 μg) were linearized at a unique *Not*I site and electroporated into *TbGPI10* or *TbGPI8* knockout *T. brucei* mutants. A clonal cell line was established by limiting dilution. Cells were maintained at 27 °C in SDM-79 medium supplemented with 10% foetal bovine serum, 7.5 μg/ml haemin, and appropriate antibiotics.

2.2. Plasmid construction

Tb927.7.6850 (TbTS) was amplified from the *T. brucei* genome by PCR using the following primers: 5′-CTCTTAAGATGGAGGAACTCCACCAACAAATGC-3′ carrying an *Afl*II site and 5′-CCATGGATCGATAACTGCACTGACGACC-3′ carrying *Nco*I and *Cla*I sites. This resulted in the amplification of an open reading frame (ORF) excluding the predicted omega site (the site cleaved by GPI-transamidase) and the GPI signal sequence at the *C*-terminus. The amplified fragment was digested with *Afl*II and *Nco*I. The *C*-terminal omega site and the GPI signal sequence of TbTS were amplified separately using the following primers: 5′-CCATGGTCTAGAGGTATCCCCGAAGGTATG-3′ carrying *Nco*I and *Xba*I sites, and 5′-TGCTCTAGATCTCAAATCGCCAACACATACATTAAG-3′ carrying *Xba*I and *Bgl*II sites. Fragments were then digested with *Xba*I and *Bgl*II. A FLAG-HAT epitope tag was amplified from pMEEB-FLAG-rPIG-W-FLAG-HAT [12] using the following primers: 5′-CTTAAGCCATGGGACTACAAGGACGACGATG-3′ carrying *Afl*II and *Nco*I sites and 5′-TCTAGACTTGTTGTGGGCATGAGCG-3′ carrying an *Xba*I site. The amplified product was then digested with *Nco*I and *Xba*I. These three fragments were ligated into an expression vector (pPPMCSzeo) digested with *Afl*II and *Bam*HI. The expression vector pPPMCSzeo was constructed from pPPMCS [8] by replacing its hygromycin resistance gene with a phleomycin resistance gene. This expression vector, designated as pPPMCSzeo-TbTS-FH, was designed to express and secrete *C*-terminally FLAG-HAT-tagged TbTS after processing of the *N*-terminal signal peptide and the *C*-terminal GPI signal sequence, when transfected into *TbGPI10* knockout mutants.

An expression vector for *Tb927.8.7350* (TbSA C2) was constructed using a similar four-part ligation. TbSA C2 was amplified using the following primer sets: 5′-CTAGTCTAGAGATGCAAAAGAAGGTACTACC-3′ carrying an *Xba*I site and 5′-CCGCGGAGATCTATGCTGACAGTAACTGGAG-3′, carrying *Sac*II and *Bgl*II sites. Fragments were then digested with *Xba*I and *Bgl*II. This fragment lacks an *N*-terminal signal peptide, but includes a *C*-terminal omega-site and a GPI signal sequence. The signal peptide fragment was amplified from the TbTS gene using the following primers: 5′-CTCTTAAGATGGAGGAACTCCACCAACAAATGC-3′ carrying an *Afl*II site and 5′-TCTAGACCATGGGCCCGCAGCCTTGGAAGTCAG-3′, carrying *Xba*I and *Nco*I sites, and was digested with *Afl*II and *Nco*I. These two fragments and the FLAG-HAT epitope tag (digested with *Nco*I and *Xba*I as above) were ligated together with pPPMCSzeo. The resultant plasmid, designated as pPPMCSzeo-FH-TbSAC2, was designed to express and secrete TbSA C2 with a FLAG-HAT epitope tag at the *N*-terminus.

Tb927.2.5280 (TbTS-like D1) was amplified using the following primer sets for the ORF excluding the predicted omega site and GPI signal sequence: 5′-CGGGGTACCTTAAGATGCGCGTTGTATACCAGCG-3′ carrying *Kpn*I and *Afl*II sites, and 5′-CATGCCATGGATCGATAGGGGTACGGAACGCGTGGTCT-3′ carrying *Nco*I and *Cla*I sites. The amplified fragment was ligated as in the pPPMCSzeo-TbTS-FH construction. The resultant plasmid, designated as pPPMCSzeo-TbTSD1-FH, was designed to express and secrete TbTS-like D1 protein carrying a FLAG-HAT epitope tag at the *C*-terminus.

TbGPI8 knockout mutants expressing a soluble form of TbTS have been generated previously [8]. In order to create a *TbGPI8* knockout mutant expressing a soluble form of TbSA C2, we constructed a vector for the expression of soluble TbSA C2 carrying a FLAG-HAT epitope tag at the *N*-terminus. To clone the mature form of the protein without the GPI signal sequence, TbSA C2 was amplified using the following primer sets: 5′-CTAGTCTAGAGATGCAAAAGAAGGTACTACC-3′ carrying an *Xba*I site, and 5′-TGCTCTAGATCTAGTTTTCATTCATCTCGTTTCC-3′ carrying *Xba*I and *Bgl*II sites. The PCR product was digested with *Xba*I and *Bgl*II, and ligated with the TbTS signal peptide fragment, the FLAG-HAT epitope tag, and pPPMCSzeo (prepared as described for pPPMCSzeo-FH-TbSAC2). The resultant plasmid, designated as pPPMCSzeo-FH-TbSAC2sol, encoded a soluble form of TbSA C2, which carried a FLAG-HAT epitope tag immediately downstream of the signal peptide. This plasmid was introduced into *TbGPI8* knockout mutant *T. brucei*.

2.3. Protein purification

The medium (typically 30 ml) containing secreted trans-sialidases was incubated with 30–40 μl of anti-FLAG agarose at 4 °C overnight, with rotary mixing. The resin was washed five times with a buffer containing 50 mM Tris–HCl buffer, pH 7.4, 150 mM NaCl, and 0.1% Tween 20, and successively with 40 mM HEPES buffer (pH 7.4). Bound enzymes were eluted using the FLAG peptide. FLAG peptide was removed from the eluent by dialysis against 40 mM HEPES buffer (pH 7.4), and protein concentrations were measured using a BCA assay (Pierce). The purities of the enzymes were determined by SDS–PAGE (7.5% gel) and silver staining. For Western blotting, purified proteins were probed with mouse anti-FLAG M2 monoclonal antibody (Sigma) followed by horseradish peroxidase-conjugated sheep anti-mouse IgG antibody (GE Healthcare), and detected by enhanced chemiluminescence (PerkinElmer Life Sciences).

2.4. Enzyme assays

Sialidase and trans-sialidase activities were measured as previously described [8,13,14], with minor modifications. For the assays of sialidase activity, the fluorogenic substrate 2′-(4-methylumbelliferyl) α-D-*N*-acetylneuraminic acid (4MU-NANA; Sigma) was added to a final concentration of 250 μM. Lactose was added in some experiments, as indicated. One unit of sialidase activity was defined as the activity that releases 1 μmol of 4MU/min. For the assays of trans-sialidase activity, enzymes were incubated at 32 °C for 14 h with 400 μM βGal-4MU as an acceptor, and 200 μM α2,3 sialyllactose (3′SL; Calbiochem) or α2,6 sialyllactose (6′SL; Calbiochem) as a donor in a buffer containing 40 mM HEPES (pH 7.4). Sialylated products were bound to Q-Sepharose Fast Flow (GE Healthcare) resin, washed with water, eluted with 1 M HCl, and hydrolysed for 30 min at 95 °C. After hydrolysis, the pH was readjusted to 9.5 and the fluorescence of released 4MU was measured using a microplate reader (excitation 365 nm, emission 450 nm). The sialylated fluorescent product was also detected by TLC (silica gel 60 F_{254}; Merck) using chloroform/methanol/water (60:40:10, v/v/v) as a developing solvent. The reaction products were detected by UV light. To examine the linkage of sialylated products, the samples were treated with α2,3 neuraminidase from *Macrobdella decora* (Calbiochem) [15], or α2,3,6,8,9 sialidase A from *Arthrobacter ureafaciens* (Prozyme), prior to TLC.

3. Results

In addition to the canonical trans-sialidase TbTS encoded by the ORF *Tb927.7.6850*, we cloned four other trans-sialidase homologs (encoded by *Tb927.5.640*, *Tb927.8.7350*, *Tb927.2.5280*, and *Tb927.7.7480*) from the *T. brucei* genome. *Tb927.5.640* and *Tb927.2.5280* encode proteins that have been designated as TbSA B and TbTS-like D1, respectively (Table 1) [11]. *Tb927.8.7350* is present in tandem with *Tb927.8.7340* in the genome. These two ORF are highly homologous, and the amino acid sequence identity of the gene products is 96%. These two proteins have been designated collectively as TbSA C [11], but here we designated the protein products of *Tb927.8.7340* and *Tb927.8.7350* as TbSA C1 and TbSA C2, respectively, in order to differentiate between these two genes more clearly. The protein encoded by *Tb927.7.7480* has not been described previously, but shows the highest homology with TbSA B (84% amino acid identity), and we therefore designated this protein as TbSA B2. CLUSTAL W multiple sequence alignment indicated that amino acid residues known to be important for the trans-sialidase function are conserved between TbSA B and TbSA B2 (data not shown). In addition, TbSA B2, like TbSA B, does not appear to contain a GPI anchoring signal, based on prediction software such as fragAnchor [16] and GPI-SOM [17] (Table 1).

It has been reported that several TbTS homologs expressed and purified from bacteria were inactive [11]. Therefore, instead of relying on bacterial expression system, we took advantage of our *T. brucei* GPI mutants, which efficiently secrete proteins with signal peptide and GPI anchoring signal [8]. We first expressed these proteins in *TbGPI10* knockout mutant under the control of the PARP promoter. We designed the cloning so that epitope tags were attached to either the *N*- or *C*-terminus of the protein after the signal peptide was removed and the GPI anchor signal was hydrolysed at the omega site in the absence of a mature GPI precursor. We investigated whether or not the resultant soluble proteins were secreted into the culture medium. As previously reported [8], medium from empty vector transformant showed a certain level of sialidase activity due to secretion of endogenous trans-sialidases (Fig. 1A). When the cells expressing canonical TbTS were used, the resultant medium showed an increase in sialidase activity, confirming that our mutant *T. brucei* cell line functions as an efficient protein expression/secretion system. Strikingly, medium from TbSA C2-expressing cells showed a significantly higher level of sialidase activity than empty vector control. In contrast, TbSA D1 expression did not resulted in an increased level of sialidase activity, suggesting that TbSA D1 is not a functional sialidase under the condition we used. Taken together, among additional TbTS homologs, TbSA C2 appears to function as a sialidase.

The use of *TbGPI10* mutant results in a significant level of background sialidase activity due to endogenous TbTS. In contrast, we have previously shown that *TbGPI8* knockout mutant transfected

Table 1
trans-Sialidase homologs in the *T. brucei* genome.

Systematic name[a]	Common name	Amino acids	Mass (kDa)	GPI anchor prediction		Reference
				fragAnchor[b]	GPI-SOM[c]	
Tb927.7.6850	TbTS	771	84.5	+	++	[6]
Tb927.7.6830	TbTSsh	427	47.4	–	–	[11]
Tb927.5.640	TbSA B	816	90.3	–	–	[11]
Tb927.7.7480	TbSA B2	816	90.2	–	–	This study
Tb927.8.7340	TbSA C1	748	81.0	++	++	[11]
Tb927.8.7350	TbSA C2	748	81.2	++	++	[11]
Tb927.2.5280	TbTS-like D1	702	77.2	++	++	[11]
Tb11.01.3240	TbTS-like D2	681	75.1	+	++	[11]
Tb927.5.440	TbTS-like E	775	84.6	–	–	[11]

[a] Bolded systematic names indicate the genes characterized in this study.
[b] (++) Highly probable; (+) potentially false positive; (–) rejected.
[c] (++) GPI-anchored; (–) not GPI-anchored or uncertain.

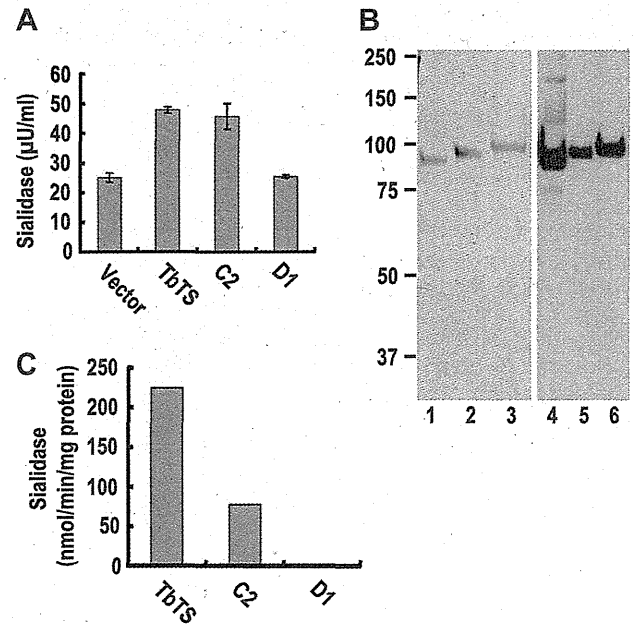

Fig. 1. Purification and sialidase activities of TbTS and its homologs. (A) *TbGPI10* knockout cells were transfected with various trans-sialidase homologs. These cells secrete trans-sialidases as soluble forms. Culture supernatants were examined for sialidase activities. Each measurement was repeated 3 times, and the average and standard deviation are shown. (B) trans-Sialidase homologs were expressed in *TbGPI8* knockout cells, purified by affinity purification, and examined for purity by SDS–PAGE and silver staining (lanes 1–3) or Western blotting (lanes 4–6). Lanes 1 and 4, TbTS; lanes 2 and 5, TbSA C2; lanes 3 and 6, TbTS-like D1. Molecular weight markers are indicated on the left (kDa). (C) Sialidase activities of purified enzymes. Each measurement was in duplicate, and averages are shown.

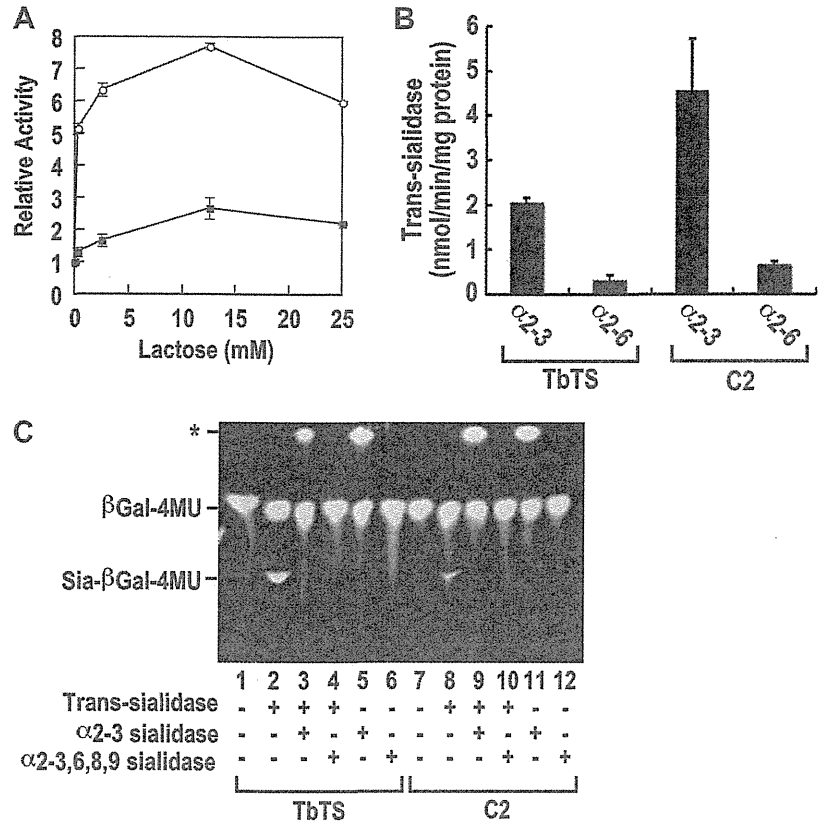

Fig. 2. trans-Sialidase activity of TbSA C2. (A) Activities of soluble forms of TbTS and TbSA C2 are enhanced by lactose. Open circle, TbTS; closed square, TbSA C2. Relative activities to those at 0 mM lactose are shown. The assay was performed in triplicate and averages and standard deviations are shown. (B) TbTS and TbSA C2 were examined for trans-sialidase reaction using α2,3 or α2,6 sialyllactose as a donor. The assay was performed in triplicate and averages and standard deviations are shown. (C) The product formed by the trans-sialidase reaction was visualised by TLC separation and fluorographic imaging. The bands denoted by asterisk in lanes 3, 5, 9 and 11 indicate free 4MU, which was apparently generated due to a β-galactosidase, a known contaminant of α2,3 neuraminidase preparations.

with empty vector does not secrete significant levels of endogenous trans-sialidases [8]. This is because the *TbGPI8* mutant cannot cleave the hydrophobic GPI anchoring signal and therefore cannot secrete unanchored proteins [8]. The culture medium of the *TbGPI8* knockout mutant is therefore devoid of endogenous trans-sialidases, which is advantageous for subsequent protein purification.

We therefore expressed secretory forms of trans-sialidase homologs in *TbGPI8* knockout mutant. Each trans-sialidase homolog carries a FLAG epitope tag, which was used to affinity-purify the secreted trans-sialidases. The use of *TbGPI8* knockout mutant and affinity purification of epitope-tagged protein allowed us to obtain a highly purified protein, which is essentially homogeneous based on silver staining of SDS–PAGE gel (Fig. 1B, left panel). These bands, which were at positions near to the predicted molecular weights, were also detected by Western blotting using anti-FLAG antibodies (Fig. 1B, right panel). Taken together, Fig. 1B excludes a possibility of co-purifying other endogenous trans-sialidase homologs and there was also no significant level of protein degradation. We examined the sialidase activity of the purified enzymes. As shown in Fig. 1C, TbTS-like D1 showed little activity, while TbSA C2 showed a significant level of activity, being consistent with the data described in Fig. 1A. We were also able to express and purify TbSA B and TbSA B2, but we could not detect enzyme activities (data not shown).

We decided to focus on TbSA C2, and examined its enzymatic characteristics. As shown in Fig. 2A, lactose-dependent enhancement of sialidase activity was observed for both TbTS and TbSA C2. Lactose can act as a surrogate acceptor for the trans-sialidase reaction, suggesting that the secreted soluble TbSA C2 may be an active trans-sialidase. In order to demonstrate the trans-sialidase activity of TbSA C2 more directly, we set up a trans-sialidase assay in which the enzyme was incubated with α2,3 or α2,6 sialyllactose (as a donor) and βGal-4MU (as an acceptor). The product Sia-βGal-4MU was purified and hydrolysed, and released 4MU was measured. As shown in Fig. 2B, TbSA C2 as well as TbTS were able to mediate the trans-sialidase reaction when α2,3 sialyllactose was provided as a donor. The α2,3 sialyllactose-dependent product formation was further demonstrated by TLC (Fig. 2C), in which the product Sia-βGal-4MU was detected in reactions containing TbSA C2 as a source of enzyme. The product was sensitive to digestion by an α2,3-specific sialidase, suggesting that the enzyme mediates the production of α2,3-linked sialic acid. Taken together, we conclude that TbSA C2 is a catalytically active α2,3 trans-sialidase.

4. Discussion

In this study, we identified a new trans-sialidase (TbSA C2 encoded by *Tb927.8.7350*) in *T. brucei*, in addition to the known trans-sialidase (TbTS encoded by *Tb927.7.6850*). We showed that TbSA C2 was an active enzyme, able to transfer α2,3-linked sialic acid from donor glycoconjugates to acceptor glycoconjugates. *Tb927.8.7350* exists in tandem with *Tb927.8.7340* in the *T. brucei* genome, and the gene products TbSA C1 and TbSA C2 are highly homologous (96% identity). We did not investigate TbSA C1 in this study, but it is likely that TbSA C1 is also an active trans-sialidase.

We did not detect any enzyme activities from the other three homologs (*i.e.* TbSA B, TbSA B2 and TbTS-like D1). Among them, TbTS-like D1 lacks the amino acid residues that are predicted to be critical for the catalytic domains of a trans-sialidase [11], and its lack of enzymatic activity is therefore consistent with its structural features.

Almost complete inhibition of trans-sialidase activity has previously been achieved with TbTS RNAi [11]. This observation suggested that TbTS was the major trans-sialidase in *T. brucei*. We demonstrated that TbSA C2 can function as a trans-sialidase. Considering the major contribution of TbTS to trans-sialidase activity, TbSA C2 might make only a minor contribution to the sialylation of GPI side chains. However, this enzyme might act on a specific structural motif within the GPI side chain, or some other, yet-unknown glycoconjugates. We hypothesize that TbSA C2 is a physiologically important enzyme, carrying out modifications critical for the growth of *T. brucei* in the fly midgut. In the light of recent reports that TbSA C2 RNAi affects sialidase activity more significantly than trans-sialidase activity, it is possible that TbSA C2 remodels the sialic acid modifications, rather than simply functioning as an additional trans-sialidase [11]. Future experiments to test the restoration of midgut infectivity of *TbGPI8* knockout mutants expressing soluble forms of both TbTS and TbSA C2 will provide further information on the biological functions of the trans-sialidase gene family in *T. brucei*.

Acknowledgments

We thank Keiko Kinoshita, Fumiko Mori, and Kana Miyanagi for assistance. This work was supported by grants from MEXT to T.K., and from the Human Frontier Science Program Organization to Y.S.M.

References

[1] I. Roditi, A. Furger, S. Ruepp, N. Schurch, P. Butikofer, Unravelling the procyclin coat of *Trypanosoma brucei*, Mol. Biochem. Parasitol. 91 (1998) 117–130.
[2] A. Treumann, N. Zitzmann, A. Hulsmeier, A.R. Prescott, A. Almond, J. Sheehan, M.A. Ferguson, Structural characterisation of two forms of procyclic acidic repetitive protein expressed by procyclic forms of *Trypanosoma brucei*, J. Mol. Biol. 269 (1997) 529–547.
[3] M.A. Ferguson, P. Murray, H. Rutherford, M.J. McConville, A simple purification of procyclic acidic repetitive protein and demonstration of a sialylated glycosyl-phosphatidylinositol membrane anchor, Biochem. J. 291 (1993) 51–55.
[4] M. Engstler, G. Reuter, R. Schauer, The developmentally regulated trans-sialidase from *Trypanosoma brucei* sialylates the procyclic acidic repetitive protein, Mol. Biochem. Parasitol. 61 (1993) 1–13.
[5] L.C. Pontes de Carvalho, S. Tomlinson, F. Vandekerckhove, E.J. Bienen, A.B. Clarkson, M.S. Jiang, G.W. Hart, V. Nussenzweig, Characterization of a novel trans-sialidase of *Trypanosoma brucei* procyclic trypomastigotes and identification of procyclin as the main sialic acid acceptor, J. Exp. Med. 177 (1993) 465–474.
[6] G. Montagna, M.L. Cremona, G. Paris, M.F. Amaya, A. Buschiazzo, P.M. Alzari, A.C. Frasch, The trans-sialidase from the African trypanosome *Trypanosoma brucei*, Eur. J. Biochem. 269 (2002) 2941–2950.
[7] K. Nagamune, T. Nozaki, Y. Maeda, K. Ohishi, T. Fukuma, T. Hara, R.T. Schwarz, C. Sutterlin, R. Brun, H. Riezman, T. Kinoshita, Critical roles of glycosylphosphatidylinositol for *Trypanosoma brucei*, Proc. Natl. Acad. Sci. USA 97 (2000) 10336–10341.
[8] K. Nagamune, A. Acosta-Serrano, H. Uemura, R. Brun, C. Kunz-Renggli, Y. Maeda, M.A. Ferguson, T. Kinoshita, Surface sialic acids taken from the host allow trypanosome survival in tsetse fly vectors, J. Exp. Med. 199 (2004) 1445–1450.
[9] K. Ohishi, K. Nagamune, Y. Maeda, T. Kinoshita, Two subunits of glycosylphosphatidylinositol transamidase, GPI8 and PIG-T, form a functionally important intermolecular disulfide bridge, J. Biol. Chem. 278 (2003) 13959–13967.
[10] S. Lillico, M.C. Field, P. Blundell, G.H. Coombs, J.C. Mottram, Essential roles for GPI-anchored proteins in African trypanosomes revealed using mutants deficient in GPI8, Mol. Biol. Cell 14 (2003) 1182–1194.
[11] G.N. Montagna, J.E. Donelson, A.C. Frasch, Procyclic *Trypanosoma brucei* expresses separate sialidase and trans-sialidase enzymes on its surface membrane, J. Biol. Chem. 281 (2006) 33949–33958.
[12] Y. Murakami, U. Siripanyapinyo, Y. Hong, J.Y. Kang, S. Ishihara, H. Nakakuma, Y. Maeda, T. Kinoshita, PIG-W is critical for inositol acylation but not for flipping of glycosylphosphatidylinositol-anchor, Mol. Biol. Cell 14 (2003) 4285–4295.
[13] S. Schrader, E. Tiralongo, G. Paris, T. Yoshino, R. Schauer, A nonradioactive 96-well plate assay for screening of trans-sialidase activity, Anal. Biochem. 322 (2003) 139–147.
[14] M. Engstler, R. Schauer, R. Brun, Distribution of developmentally regulated trans-sialidases in the Kinetoplastida and characterization of a shed trans-sialidase activity from procyclic *Trypanosoma congolense*, Acta Trop. 59 (1995) 117–129.
[15] M.Y. Chou, S.C. Li, Y.T. Li, Cloning and expression of sialidase L, a NeuAcα2 → 3Gal-specific sialidase from the leech, *Macrobdella decora*, J. Biol. Chem. 271 (1996) 19219–19224.
[16] G. Poisson, C. Chauve, X. Chen, A. Bergeron, FragAnchor: a large-scale predictor of glycosylphosphatidylinositol anchors in eukaryote protein sequences by qualitative scoring, Genom. Proteom. Bioinf. 5 (2007) 121–130.
[17] N. Fankhauser, P. Maser, Identification of GPI anchor attachment signals by a Kohonen self-organizing map, Bioinformatics 21 (2005) 1846–1852.

Published June 13, 2011

JEM

Article

ATF6β is a host cellular target of the *Toxoplasma gondii* virulence factor ROP18

Masahiro Yamamoto,[1,3] Ji Su Ma,[1,3] Christina Mueller,[5] Naganori Kamiyama,[1,3] Hiroyuki Saiga,[1,3] Emi Kubo,[1] Taishi Kimura,[1,3] Toru Okamoto,[4] Megumi Okuyama,[1,3] Hisako Kayama,[1,3] Kisaburo Nagamune,[6] Seiji Takashima,[2] Yoshiharu Matsuura,[4] Dominique Soldati-Favre,[5] and Kiyoshi Takeda[1,3]

[1]Department of Microbiology and Immunology and [2]Department of Cardiovascular Medicine, Graduate School of Medicine; [3]Laboratory of Mucosal Immunology, World Premier International Research Center Immunology Frontier Research Center; and [4]Department of Molecular Virology, Research Institute for Microbial Diseases; Osaka University, Suita, Osaka 565-0871, Japan
[5]Department of Microbiology and Molecular Medicine, University Medical Center, University of Geneva, 1211 Geneva 4, Switzerland
[6]Department of Parasitology, National Institute of Infectious Diseases, Shinjuku-ku, Tokyo 162-8640, Japan

The ROP18 kinase has been identified as a key virulence determinant conferring a high mortality phenotype characteristic of type I *Toxoplasma gondii* strains. This major effector molecule is secreted by the rhoptries into the host cells during invasion; however, the molecular mechanisms by which this kinase exerts its pathogenic action remain poorly understood. In this study, we show that ROP18 targets the host endoplasmic reticulum–bound transcription factor ATF6β. Disruption of the *ROP18* gene severely impairs acute toxoplasmosis by the type I RH strain. Because another virulence factor ROP16 kinase modulates immune responses through its N-terminal portion, we focus on the role of the N terminus of ROP18 in the subversion of host cellular functions. The N-terminal extension of ROP18 contributes to ATF6β-dependent pathogenicity by interacting with ATF6β and destabilizing it. The kinase activity of ROP18 is essential for proteasome-dependent degradation of ATF6β and for parasite virulence. Consistent with a key role for ATF6β in resistance against this intracellular pathogen, ATF6β-deficient mice exhibit a high susceptibility to infection by ROP18-deficient parasites. The results reveal that interference with ATF6β-dependent immune responses is a novel pathogenic mechanism induced by ROP18.

CORRESPONDENCE
Kiyoshi Takeda:
ktakeda@ongene.med.osaka-u.ac.jp

Abbreviations used: BMDC, BM-derived DC; ERAD, ER-associated degradation; GST, glutathione *S*-transferase; HA, hemagglutinin; HFF, human foreskin fibroblast; IRG, immunity-related GTPase; KD, kinase dead; MOI, multiplicity of infection; MPA, mycophenolic acid; PFA, paraformaldehyde; PV, parasitophorous vacuole; PVM, PV membrane; UPR, unfolded protein response; UPRE, UPR element.

Toxoplasma gondii causes life-threatening toxoplasmosis in immunocompromised individuals such as those suffering from AIDS or being treated by chemotherapy (Montoya and Remington, 2008). As a member of the phylum of Apicomplexa, *T. gondii* is an obligate intracellular parasite, defined by the presence of an apical complex including secretory organelles such as rhoptries and micronemes (Joynson and Wreghitt, 2001). During invasion, *T. gondii* delivers numerous effector molecules into the forming parasitophorous vacuole (PV) and the host cytoplasm to co-opt the host cell for growth and survival (Boothroyd and Dubremetz, 2008).

T. gondii is divided into three major lineages (types I, II, and III) in addition to exotic strains (Ajzenberg et al., 2004; Dardé, 2008). Although type II parasites are the most prevailing opportunistic strains, infection with type I strains appears to be responsible for encephalitis in AIDS patients, ocular toxoplasmosis, and congenital hydrocephalus, whereas infection with type III strains seldom results in disease manifestations (Howe and Sibley, 1995; Boothroyd and Grigg, 2002). In terms of the strain-dependent phenotypes, virulence in mice has been well characterized, although the median lethal dose of type II or III parasites ranges from 10^2 to 10^5, and the lethal dose of the most virulent type I strain is one (10^0) parasite (Sibley and Boothroyd, 1992; Sibley and Howe, 1996;

T. Okamoto's present address is The Walter and Eliza Hall Institute of Medical Research, Parkville, Victoria 3052, Australia.

The Rockefeller University Press $30.00
J. Exp. Med. Vol. 208 No. 7 1533-1546
www.jem.org/cgi/doi/10.1084/jem.20101660

Supplemental Material can be found at:
http://jem.rupress.org/content/suppl/2011/06/12/jem.20101660.DC1.html

Published June 13, 2011

Dubremetz, 2007). Previous forward genetic studies, in which types I/II and III were intercrossed to explore genes responsible for virulence, culminated in the identification of *ROP18* as the dominant candidate gene (Saeij et al., 2006; Taylor et al., 2006).

ROP18 is a Ser/Thr kinase related to the ROP2 subfamily, secreted by the rhoptries into the PV and host cytosol. Its action as effector molecule is anticipated to modulate host factors by an as yet unknown mechanism (El Hajj et al., 2006; Taylor et al., 2006; Dubremetz, 2007). Most recently, ROP18 has been shown to target a member of IFN-inducible small GTPases (immunity-related GTPases [IRGs]), Irgb6 (Fentress et al., 2010; Steinfeldt et al., 2010), indicating that interference with the innate function of Irgb6 is a key mechanism by which ROP18 mediates virulence at an early stage after infection. ROP16, another ROP2 subfamily member, was previously identified as virulence determinant, distinguishing how type I/III and II strains activate Stat3/6 during parasite

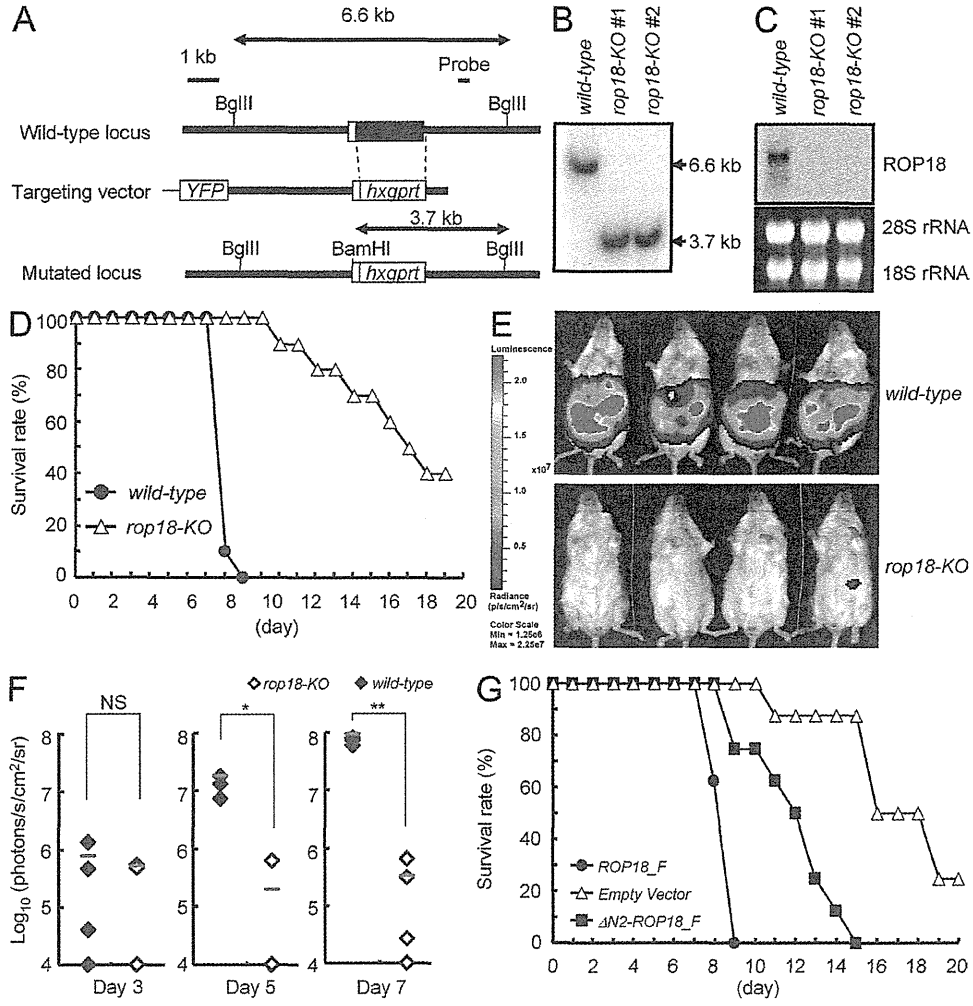

Figure 1. The N terminus of ROP18 is required for acute virulence in type I *T. gondii*. (A) The structure of the *ROP18* gene, the targeting vector, and the predicted disrupted gene. Closed boxes denote the exons. (B) Southern blot analysis of WT or two lines of *rop18-KO* parasites. 30 µg total genomic DNA was extracted from parasites, digested with BglII–BamHI, electrophoresed, and hybridized with the radiolabeled probe indicated in A. Southern blotting yielded a single 6.6-kb band for the WT and a 3.7-kb band for the disrupted locus. (C) Northern blot analysis on 10 µg total parasite RNA separated on a gel, transferred to a nylon membrane, and hybridized with ROP18 probe. The 28S and 18S ribosomal RNA is shown as the loading control (bottom). (D) BALB/c mice ($n = 10$) were infected with 10^3 WT or *rop18-KO* parasites, and the survival rates were monitored for 20 d. (E) BALB/c mice ($n = 4$) were infected with 10^3 WT or *rop18-KO* luciferase-expressing parasites, and the progress of infection was assessed by bioluminescence imaging at day 6 after infection. The color scale indicates photon emission during a 60-s exposure. (F) Total photon emission analysis from BALB/c mice ($n = 4$) infected with 10^3 WT or *rop18-KO* luciferase-expressing parasites at days 3, 5, or 7 after infection. Abdominal photon emission was assessed during a 60-s exposure. The red bars show means of the four samples. *, $P < 0.05$; **, $P < 0.001$. (G) BALB/c mice ($n = 8$) were infected with 10^3 *rop18-KO* parasites complemented with the indicated vectors, and the survival rates were monitored for 20 d. (B–G) Data are representative of two independent (B, C, E, and F) or cumulative percentages of two independent (D and G) experiments.

Published June 13, 2011

infection (Saeij et al., 2006, 2007). Subsequently, this effector molecule was shown to directly phosphorylate Stat3 and Stat6, and the N-terminal extension of ROP16 was demonstrated to play a key role in the interaction with the substrates (Yamamoto et al., 2009; Ogawa et al., 2010; Ong et al., 2010). Like ROP16, ROP18 exhibits an uncharacterized N-terminal extension (El Hajj et al., 2006).

To explore the function of the N terminus of ROP18, we first generated ROP18-deficient type I parasites and confirmed the in vivo significance of ROP18 in the type I parasite–mediated virulence. Complementation experiments showed that the N-terminal portion of ROP18 is required for the full recovery of virulence in *rop18-KO* parasites. A yeast two-hybrid screening and biochemical experiments found that the host factor ATF6β is a binding partner with the N-terminal extension of ROP18. This association led to a proteasome-dependent degradation of ATF6β in a kinase activity–dependent manner. Consistent with a defensive function of ATF6β against the parasite, ATF6β-deficient mice were generated and shown to be highly susceptible to *rop18-KO* but not WT parasites. Collectively, these results identified ATF6β as one of the host cellular factors targeted by ROP18 in the context of acute pathogenesis by the type I *T. gondii* strain.

RESULTS

The N terminus of ROP18 is involved in acute virulence in type I parasites

To determine whether ROP18 contributes to the high mortality rate of type I strains in mice, we disrupted the *ROP18* gene in the type I RH strain by reverse genetics and isolated several independent clones (Fig. 1, A and B). Northern blot analysis confirmed the absence of *ROP18* messenger RNAs in the clones (Fig. 1 C). The parasite lytic cycle as measured by plaque assay and intracellular growth on human foreskin fibroblasts (HFFs) was unaffected in these mutants as compared with WT parasites (Fig. S1, A and B). The recruitment of host organelles such as the mitochondria and ER around the PV was unaltered (unpublished data). We first challenged BALB/c mice with WT or *rop18-KO* parasites and monitored animal survival for 20 d. All mice infected with WT parasites died within 9 d. In contrast, mice infected with *rop18-KO* parasites showed a considerably lower mortality rate (Fig. 1 D). Luciferase-expressing WT or *rop18-KO* parasites were generated to visualize the in vivo parasite burden in BALB/c mice. A significantly stronger signal was detected in the ventral side of mice infected with WT parasites than those with *rop18-KO* parasites (Fig. 1 E). Moreover, the photon flux measurement during the course of infection increased notably faster and demonstrated a two log difference between WT and *rop18-KO* parasites at 7 d after infection (Fig. 1 F). Given the importance of the N-terminal extension for ROP16, we complemented *rop18-KO* parasites with full-length Flag-tagged (F) ROP18 (*ROP18_F* strain), the ROP18 mutant deleted in residues 147–164 of the N-terminal portion (*ΔN2-ROP18_F* strain), or the empty vector (*Empty vector* strain) and tested the recovery of the acute virulence phenotype (Fig. S2, A and B). Expression of ROP18_F fully restored acute virulence, whereas the *Empty vector* parasites exhibited an avirulent phenotype comparable with the parental *rop18-KO* parasites. The recovery of the virulence in *ΔN2-ROP18* parasites was only partial compared with the *ROP18_F* strain (Fig. 1 G). These data formally establish that ROP18 is a virulence factor of acute toxoplasmosis in type I strain and highlight the important contribution of the N-terminal extension of ROP18 for the full manifestation of the virulence phenotype.

Enhanced type I immune responses in mice infected with *rop18-KO* parasites

We next compared type I immune responses in the infected BALB/c mice because IFN-γ, mainly produced by Th1-polarized CD4 and CD8 T cells, plays a critical role in the control of acute toxoplasmosis (Subauste and Remington, 1991; Shirahata et al., 1994; Yap and Sher, 1999). 6 d after infection, CD4 and CD8 T cells from the spleens of mice demonstrating no abnormalities in appearance and no alteration in splenic cellularities and were tested for IFN-γ production by anti-CD3 treatment (Fig. S3, A–C). Compared with T cells from mice infected with WT parasites, CD4 and CD8 T cells from those infected with *rop18-KO* parasites displayed dramatically higher IFN-γ production in response to anti-CD3 (Fig. 2, A and B). To analyze antigen-specific IFN-γ production, we next compared the production from T cells stimulated with heat-killed *T. gondii* in the presence of DCs. Even in this condition, CD4 and CD8 T cells from mice infected with *rop18-KO* parasites produced higher concentrations of IFN-γ than those infected with WT parasites (Fig. 2, A and B). Collectively, these results show that ROP18 critically contributes to the suppression of the host type I immunity during infection with the virulent type I strain.

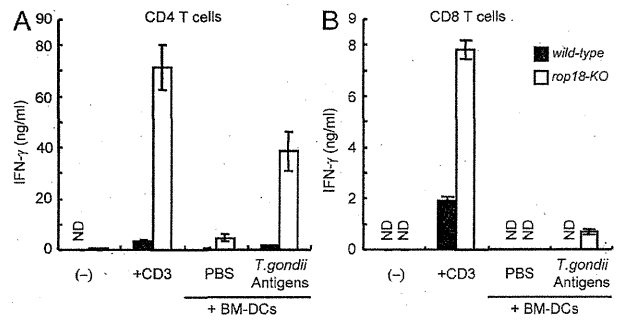

Figure 2. Enhanced IFN-γ production from T cells in mice infected with *rop18-KO* parasites. (A and B) CD4 (A) or CD8 (B) T cells from BALB/c ($n = 3$) mice were cultured in the presence of 5 µg/ml plate-bound anti-CD3 for 24 h or in the presence or absence of *T. gondii* antigen–pulsed BMDCs for 24 h. Concentration of IFN-γ in the culture supernatants was measured by ELISA. Indicated values are means ± SD of triplicates. Data are representative of three independent experiments. ND, not detected.

Published June 13, 2011

JEM

ROP18 interacts with ATF6β and mediates its degradation

The N-terminal extension of ROP16 interacts with the host factors Stat3/Stat6 (Yamamoto et al., 2009; Ogawa et al., 2010). Therefore, a yeast two-hybrid screening was undertaken to identify potential host partners interacting with the N-terminal portion of ROP18 (Nt-ROP18). ATF6β, a component of the ER membrane–bound transcription factor implicated in stress response, was found as the predominant hit, and its association with Nt-ROP18 was first confirmed in yeast cells (Fig. 3 A). Moreover, Nt-ROP18 and ATF6β failed to interact with SV40 large T antigen and p53 used as negative controls, respectively, demonstrating that Nt-ROP18 specifically associates with ATF6β in yeast (Fig. S4 A). To further assess the specificity of this interaction, we expressed Flag-tagged ROP18 lacking its signal peptide (Δ27-ROP18_F) or a larger N-terminal deletion of ROP18 (Δ240-ROP18_F) together with hemagglutinin (HA)-tagged ATF6β in mammalian 293T cells. Interestingly, we failed to detect an interaction between Δ27-ROP18_F and HA-ATF6β, but we noticed that overexpression of Δ27-ROP18_F but not Δ240-ROP18_F resulted in a dramatic reduction in the level of HA-ATF6β (Fig. 3 B). To determine whether parasite infection also caused a drop in HA-ATF6β levels, 293T cells expressing HA-ATF6β fused to CFP (with a self-cleavage signal [T2A] in between to produce the same level of both proteins) were similarly infected with WT or *rop18-KO* parasites (Fig. S4 B). The level of ATF6β protein was consistently reduced in cells infected with WT but not with *rop18-KO* parasites (Fig. 3 C). Moreover, Δ27-ROP18_F but not Δ240-ROP18_F decreased the ATF6β level in a dose-dependent fashion in dually transfected 293T cells (Fig. 3 D). ATF6β is a component of the ER stress response transcription factor that activates expression of genes harboring an unfolded protein response

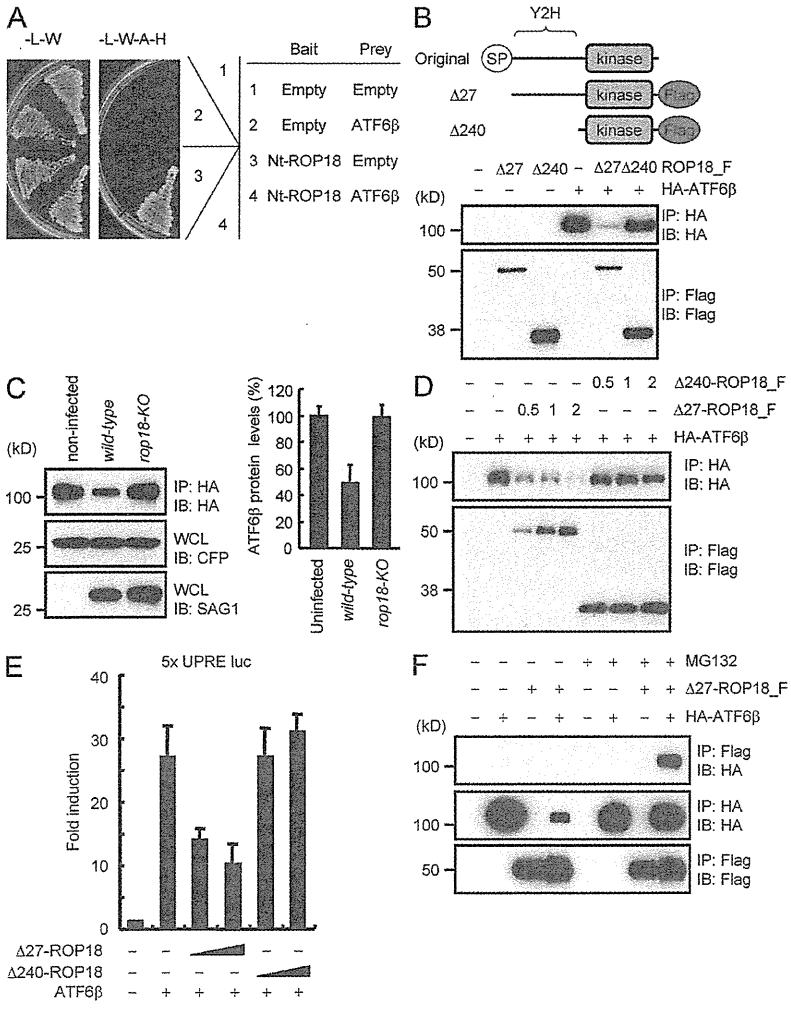

Figure 3. Identification of ATF6β as a ROP18-interacting protein. (A) Plasmids expressing Nt-ROP18 fused to the GAL4 DNA-binding domain or an empty vector were cotransfected with a plasmid expressing ATF6β fused to the GAL4 transactivation domain or an empty vector. Interactions were detected by the ability of cells to grow on medium lacking Ade, Trp, Leu, and His (-L-W-A-H). Growth of cells on plates lacking Trp and Leu (-L-W) was indicative of the efficiency of the transfection. (B) Lysates of 293T cells transiently cotransfected with 2 μg of the indicated Flag-tagged ROP18 and/or 2 μg HA-tagged ATF6β expression vectors were immunoprecipitated with the indicated antibodies and detected by Western blot with the indicated antibodies. The top images denote the structure of ROP18 variants used in this study. WT, original ROP18; SP, signal peptide; Y2H, the region used as the bait in the yeast two-hybrid screen. (C) The 293T cells transfected with 0.1 μg plasmids for tandem expression of HA-tagged ATF6β and T2A-CFP were infected with the indicated parasites at an MOI of 10. 24 h after infection, the cells were lysed and subjected to Western blot or immunoprecipitation (IP) with anti-HA (left). The expression levels of HA proteins were normalized against CFP (right). Error bars represent means ± the variation range of duplicates. IB, immunoblot; WCL, whole cell lysates. (D) Lysates of 293T cells transiently cotransfected with the indicated volumes of the Flag-tagged Δ27- or Δ240-ROP18 and/or 2 μg HA-tagged ATF6β expression vectors were immunoprecipitated with the indicated antibodies and detected by Western blot with the indicated antibodies. (E) 293T cells were transfected with the ATF6β-dependent luciferase reporter together with the indicated expression vectors. Luciferase activities were expressed as fold increases over the background levels shown by lysates prepared from mock-transfected cells. Error bars represent means ± SD of triplicates. (F) Lysates of 293T cells transiently cotransfected with 2 μg Flag-tagged ROP18 and/or 2 μg HA-tagged ATF6β expression vectors in the absence or presence of 10 μM MG132 for the last 12 h were immunoprecipitated with the indicated antibodies and detected by Western blot. (A–F) Data are representative of three (B and D–F) and two (A and C) independent experiments.

Published June 13, 2011.

(UPR) element (UPRE) in their promoters (Wang et al., 2000; Yoshida et al., 2001). Overexpression of HA-ATF6β resulted in the activation of a UPRE-containing luciferase reporter in 293T cells; however, the coexpression of Δ27-ROP18_F but not Δ240-ROP18_F down-regulated the ATF6β-dependent activation in a dose-dependent manner (Fig. 3 E). To determine whether the ROP18-dependent decrease in ATF6β protein level is mediated by the proteasome, HA-ATF6β was coexpressed with Δ27-ROP18_F in the presence of the proteasome inhibitor MG132. Under this condition, the level of ATF6β was stabilized, and the interaction between Δ27-ROP18 and ATF6β could be monitored by coimmunoprecipitation (Fig. 3 F). Together, these data support the view that ROP18 associates with ATF6β and targets it to a proteasome-dependent degradation pathway.

The kinase activity of ROP18 is required for ATF6β degradation

ROP18 was previously shown to be a secreted active protein kinase in vitro and in vivo (Taylor et al., 2006; El Hajj et al., 2007). To assess whether the kinase activity of ROP18 plays a role in type I parasite–mediated pathogenicity, we complemented the *rop18-KO* parasites with WT (ROP18_F) or kinase-dead (KD; KD-ROP18_F) constructs (Fig. S2, B and C) and tested the virulence of the corresponding parasites in BALB/c mice (Fig. 4 A). Mice infected with *ROP18_F* resulted in 100% lethality within 10 d. In contrast, most of mice infected with *KD-ROP18_F* survived throughout the tested period. These results are consistent with a previous study, which reported that an avirulent type III strain expressing the *ROP18* but not the KD form of the type I strain can acquire virulence, pointing out the essential role of kinase activity of ROP18 for acute virulence (Taylor et al., 2006). To determine whether the kinase activity is involved in the ROP18-mediated degradation of ATF6β, mammalian expression vectors for KD-ROP18_F, ATF6β, and UPRE-containing luciferase reporter were cotransfected into 293T cells and followed by luciferase assays (Fig. 4 B). Overexpression of KD-ROP18_F failed to suppress ATF6β-mediated gene activation. Moreover, the

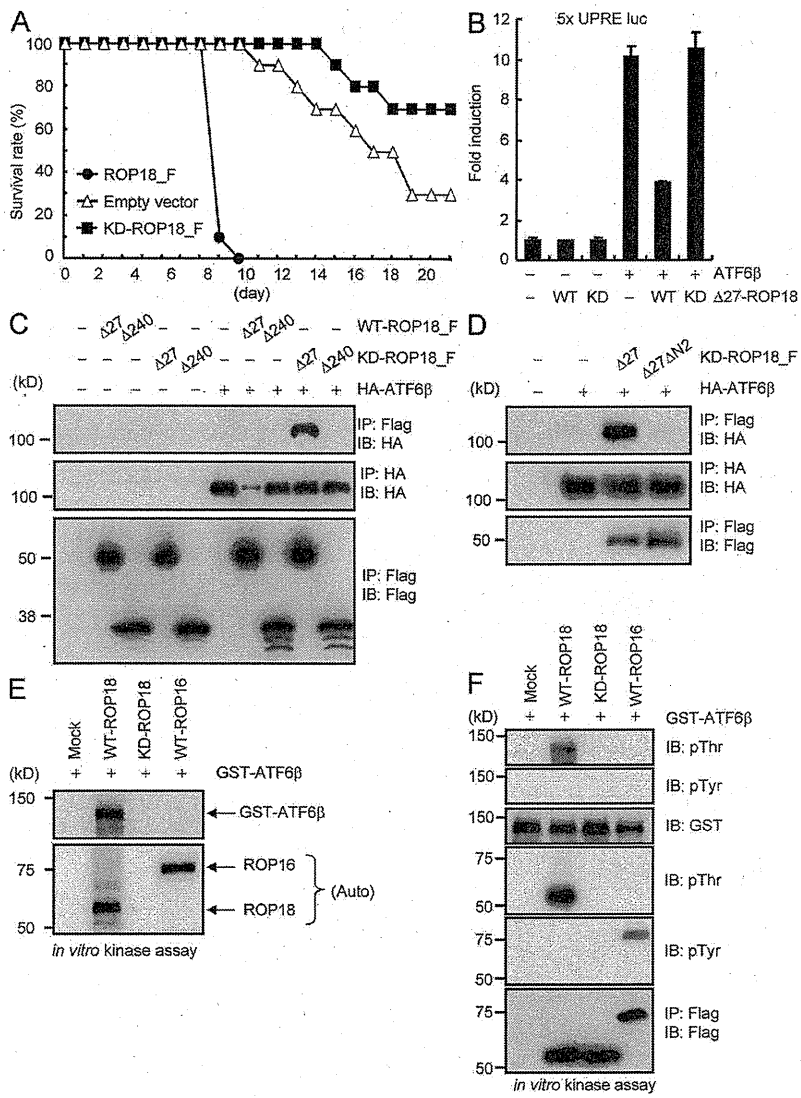

Figure 4. Essential role of ROP18 kinase activity in ATF6β degradation. (A) BALB/c mice ($n = 8$) were infected with 10^3 *rop18-KO* parasites complemented with the indicated vectors, and the survival rates were monitored for 20 d. (B) 293T cells were transfected with the ATF6β-dependent luciferase reporter together with the indicated expression vectors. Luciferase activities were expressed as fold increases over the background levels as shown by lysates prepared from mock-transfected cells. Error bars represent means ± SD of triplicates.
(C and D) Lysates of 293T cells transiently cotransfected with 2 µg of the indicated Flag-tagged ROP18 and/or 2 µg of HA-tagged ATF6β expression vectors were immunoprecipitated with the indicated antibodies and detected by Western blot. (E and F) 293T cells were transiently transfected with Flag-tagged ROP18WT, ROP18KD, or ROP16WT. Cell lysates were immunoprecipitated with anti-Flag and subjected to an in vitro kinase reaction in the presence of GST-ATF6β. Proteins were separated on SDS-PAGE, followed by autoradiography (E) or Western blot (F) to analyze ATF6β phosphorylation or the autophosphorylation of ROP18 and ROP16. For the detection of phosphorylated or unphosphorylated GST-ATF6β and Flag-tagged proteins by Western blot, anti-pThr/anti-pTyr, anti-GST, and anti-Flag were used, respectively. IB, immunoblot; IP, immunoprecipitation. (A–F) Data are representative of three (B) or two (A and C–F) independent experiments.